Biomaterials Advances 183 (2026) 214762

Contents lists available at ScienceDirect

Biomaterials Advances

journal homepage: www.journals.elsevier.com/materials-science-and-engineering-c

Thermo-responsive *in situ* hydrogel enables superior rectal administration and local efficacy of 5-ASA in inflammatory bowel disease

Elena Giuliano [a,1], Angela Costagliola di Polidoro [b,1], Agnese Gagliardi [a], Domenico Sorrentino [c], Emanuela Longo [a], Sandra Albanese [b], Francesco Napolitano [c,d], Valeria Gaetano [a], Antonella Zannetti [b,*], Donato Cosco [a,*]

[a] Department of Health Sciences, University of Catanzaro "Magna Græcia", Campus Universitario "S. Venuta", I-88100, Catanzaro, Italy
[b] Institute of Biostructures and Bioimaging, National Research Council (IBB-CNR), Napoli, 80145, Italy
[c] CEINGE-Biotecnologie Avanzate Franco Salvatore, 80145, Napoli, Italy
[d] Department of Veterinary Medicine and Animal Production, University of Naples Federico II, 81037, Napoli, Italy

ARTICLE INFO

Keywords:
5-ASA
IBD
Hydrogels
Poloxamer 407
Rectal administration

ABSTRACT

Inflammatory bowel disease (IBD) is a chronic, relapsing inflammatory disorder of the gastrointestinal tract that severely compromises quality of life. First-line therapy with 5-aminosalicylic acid (5-ASA) is limited by poor aqueous solubility, rapid upper gastrointestinal absorption and suboptimal colonic bioavailability. Although rectal administration targets the inflamed mucosa directly, conventional suppositories and enemas often reduce adherence due to discomfort and low acceptability.

A thermo-sensitive *in situ* gelling hydrogel based on poloxamer 407 (P407) is designed to address these limitations. Exploiting its amphiphilic architecture and reversible sol–gel transition at physiological temperature, P407 enables efficient encapsulation of 5-ASA, enhances mucosal adhesion and sustains local drug release. The optimized formulation demonstrates an ideal gelation profile, high muco-adhesive strength, suitable mechanical resistance, excellent injectability and spreadability, preserving the antioxidant properties of 5-ASA. The drug release profile was prolonged, even under acidic pH conditions. In an inflamed intestinal co-culture model, P407-5-ASA hydrogels markedly reduce macrophage infiltration and TNF-α secretion. In a dextran sodium sulfate-induced murine colitis model, the formulation achieves higher colonic accumulation, prolonged residence time and significantly enhanced anti-inflammatory efficacy of 5-ASA.

These results underscore the potential of P407-based hydrogels as a high-performance, patient-friendly platform for localized treatment of IBD.

1. Introduction

Inflammatory Bowel Disease (IBD) comprises a group of chronic, multifactorial inflammatory conditions of the gastrointestinal tract (GIT), resulting from a complex interplay between genetic susceptibility, environmental factors, gut microbiota dysbiosis and dietary influences [1,2].

The two main forms of IBD are Crohn's disease (CD) and ulcerative colitis (UC). UC primarily affects the colon and rectum, whereas CD may involve any portion of the GIT and is typically characterized by a transmural pattern of inflammation and a discontinuous (patchy) distribution [3].

Both disorders are associated with serious clinical manifestations, such as abdominal pain, diarrhea, and malnutrition, which not only strongly impact patients' quality of life but also represent significant challenges for the healthcare systems [4]. Additionally, IBD is recognized as a significant risk factor for the development of colorectal cancer, which can subsequently require surgical interventions such as a colostomy [3].

Consequently, the therapeutic goals to be reached for the treatment of IBD focus on inducing and maintaining remission, promoting mucosal healing, preventing surgical interventions, and reducing the risk of cancer associated with chronic inflammation [4,5].

Current therapeutic options include the use of aminosalicylates,

* Corresponding authors.
E-mail addresses: antonella.zannetti@cnr.it (A. Zannetti), donatocosco@unicz.it (D. Cosco).
[1] These authors equally contributed to this paper.

https://doi.org/10.1016/j.bioadv.2026.214762
Received 2 December 2025; Received in revised form 24 January 2026; Accepted 3 February 2026
Available online 5 February 2026

corticosteroids, antibiotics, immunosuppressants and monoclonal antibodies. Among them, 5-aminosalicylic acid (5-ASA) is generally considered the first-line treatment, especially in cases of UC [1,6–9]. 5-ASA, also known as mesalamine or mesalazine, is an anti-inflammatory drug that inhibits the release of inflammatory mediators and reduces colonic mucosal inflammation by blocking the synthesis of prostaglandins and leukotrienes [10]. It also acts as a scavenger of reactive oxygen species, which are involved in the pathogenesis of IBD, neutrophil dysfunction, and the activity of cyclooxygenase and lipoxygenase enzymes [11]. 5-ASA can be administered orally, rectally, or intravenously. However, its therapeutic efficacy is limited by poor water solubility, a low dissolution rate, and rapid absorption in the upper GIT. These factors limit its availability in the colon and may cause side effects such as nephrotic syndrome and hepatitis [12]. Therefore, improving its solubility by innovative formulations is crucial to enhance its efficacy, minimizing the potential adverse effects [13].

Rectal drug administration offers several advantages with respect to oral and parenteral routes as a consequence of the direct application of the bioactives to the site of inflammation and the rapid relief of adverse symptoms [14]. This route also bypasses the first-pass hepatic metabolism, thereby enhancing bioavailability and reducing the risk of systemic side effects [15]. Moreover, rectal administration is particularly beneficial for patients who are unable to swallow oral formulations, such as pediatric, geriatric, unconscious, or uncooperative individuals, and is generally less painful and more acceptable than injections [16–18]. Nevertheless, patient discomfort and low acceptance associated with solid suppositories and liquid enemas often compromise treatment adherence [19].

These limitations can be addressed using hydrogel-based delivery systems, which are three-dimensional crosslinked polymeric networks characterized by high water content and tunable physicochemical properties [20]. Among them, *in situ* thermo-sensitive hydrogels, undergo a sol-gel transition at body temperature, ensuring improved mucosal adhesion, prolonged drug retention at the target site and greater patient comfort [14]. Upon rectal administration, the hydrogel rapidly interacts with the mucosal surface and it then gradually degrades under the influence of intestinal mucus, enabling the sustained release of the encapsulated active compounds [21].

Poloxamer 407 (P407), commercially known as Pluronic® F127 and approved by both the U.S. Food and Drug Administration (FDA) and the European Medicines Agency (EMA) as an excipient for oral, ophthalmic, and topical formulations, has been widely employed in biomedical and pharmaceutical applications due to its excellent biocompatibility, thermo-responsive properties and remarkable capacity to encapsulate poorly water-soluble drugs [22,23].

P407 is a triblock copolymer made up of a hydrophobic polyoxypropylene (POP) core flanked by two hydrophilic polyoxyethylene (POE) chains. One of the most significant features of this copolymer is its ability to undergo a reversible sol-gel transition in aqueous media. At low temperatures, P407 exists as a free-flowing liquid, whereas upon heating, it transforms into a gel-like structure [22].

Furthermore, thanks to its amphiphilic nature, P407 spontaneously forms micellar structures in aqueous solutions, allowing the encapsulation of poorly water-soluble compounds such as 5-ASA without the need of organic solvents [24–26].

Our research team recently demonstrated that the inclusion of rutin, a poorly water-soluble molecule known for its antioxidant and anti-inflammatory properties, into the copolymeric matrix significantly enhanced its wound healing efficacy, resulting in a substantial reduction in wound size compared to the drug administered in its free form [27]. This improved therapeutic effect is primarily attributed to the ability of the hydrophobic segments of P407 to efficiently encapsulate and retain the bioactive compound, combined with its intrinsic capacity to modulate the inflammatory response and stimulate growth factor expression, thereby actively supporting the wound healing process. Furthermore, its thermo-responsive behavior facilitates formulation handling and enables convenient and effective topical application [24,27].

The thermo-responsive behavior of P407, combined with its ability to improve the drug solubility, prolong mucosal retention of the bioactives and modulate the inflammatory response, make it a conceivable material to be employed for the local delivery of 5-ASA.

The aim of this study was to develop a simple *in situ* gelling drug delivery system characterized by suitable mechanical strength and rheological properties for the local treatment of IBD. The formulations were prepared using the well-established cold method, which is straightforward, rapid, and does not require a specific equipment or complex techniques - an advantage that facilitates their potential industrial scale-up [22,28].

The impact of increasing 5-ASA concentrations up to the maximum solubilization capacity of the 20% (w/w) P407-based matrix on its physico-chemical and rheological properties was thoroughly investigated. In detail, micro- and dynamic rheology and the drug release profiles were analyzed. Additional evaluations, including spreadability, gel strength, Fourier transform infrared spectroscopy (FT-IR) analysis and the DPPH assay were carried out.

Furthermore, in this study, the P407-5-ASA formulation was characterized in cellular and murine models of IBD to evaluate its anti-inflammatory effects. To this end, we developed an optimized *in vitro* model of inflamed colon epithelium using co-cultures between polarized M1 macrophages and human colon adenocarcinoma Caco-2 cell line cells differentiated into enterocyte-like cells. These can form a polarized monolayer of cells that exhibit many of the morphological and functional characteristics of small intestine enterocytes, including the development of microvilli. In addition, the mucoadhesive properties and time-release capacity of P407-5-ASA, as well as its improved therapeutic efficacy, were tested in a mouse model of acute colitis induced by sodium dextran sulfate (DSS).

2. Materials and methods

2.1. Materials

Mesalazine (5-aminosalicylic acid, 5-ASA), poloxamer 407 (P407, trademark Pluronic® F127, molecular weight: 12,600 Da), 1,1-diphenyl-2-picrylhydrazy (DPPH), and phosphate-buffered saline (PBS) tablets were obtained from Merck (Milan, Italy).

Cellulose membrane Spectra/Por (molecular weight cut-off 3500 Da), used for the *in vitro* drug release experiments, were purchased from Spectrum Laboratories Inc. (Eindhoven, The Netherlands). All other materials and solvents used in this investigation were of analytical grade (Carlo Erba, Milan, Italy). Deionized double-distilled water was used throughout the study.

2.2. Development and characterization of an in situ gelling enema loaded with 5-ASA

2.2.1. Preparation of thermosensitive hydrogels

P407-based hydrogels were prepared following the “cold method” [28]. Briefly, P407 (20%, w/w) was dissolved in distilled water under constant stirring at 4 °C until a clear and homogeneous mixture was obtained. Successively, 5-ASA was added (0.1–0.5%, w/w), and the obtained formulations were kept overnight at the same temperature to ensure complete drug dispersion. The resulting systems were stored at 4 °C.

2.2.2. Rheological analysis and in vitro mucoadhesion assessment

The microrheological properties of P407-based hydrogels were evaluated using a Rheolaser® Master (Formulaction, Toulouse, France) based on diffusing wave spectroscopy (DWS). This technique analyses the Brownian motion of particles, which is directly influenced by the viscoelastic structure of the sample [29]. For each measurement, 20 mL

of the liquid formulation containing 5-ASA was placed into the sample holder, preheated to 37 °C. The analysis was performed at the same temperature for 30 min to determine the mean square displacement (MSD) of the particles. The MSD curve provides insights into the material's microstructure: lower slopes indicate elastic behavior, while higher slopes correspond to viscous behavior. From the MSD data, key microrheological parameters, *i.e.* Elasticity Index (EI) and Solid-Liquid Balance (SLB), were calculated using Rheosoft Master 1.4.0 software [30,31].

Rheological measurements were performed using a Kinexus® Pro rotational rheometer (Malvern Panalytical Ltd., England) equipped with a cone-plate geometry (40 mm diameter, 2° angle) and a Peltier system for temperature control. A solvent trap was used to prevent evaporation. Each liquid sample was carefully applied to the lower plate using a spatula and allowed to equilibrate for 10 min before testing [24]. Data acquisition and analysis were managed with rSpace software.

Steady-state flow tests were performed at low temperature (10 °C) and physiological temperature (37 °C) to assess the shear-thinning behavior of the systems. Viscosity was measured as a function of shear rate, ranging from 0.1 to 100 s^{-1}.

An amplitude sweep test (0.1–100 Pa) was conducted to identify the linear viscoelastic region (LVR), characterized by a shear-independent plateau. Frequency sweep tests were then performed within this region, applying a constant stress of 1 Pa, across a frequency range of 10 to 0.1 Hz, to evaluate the storage modulus (G′), loss modulus (G″) and phase angle (δ) [28].

The sol-gel transition temperature ($T_{sol\text{-}gel}$) was determined using dynamic rheological measurements through a temperature sweep test performed from 10 to 40 °C, with a heating rate of 2 °C/min (1 Hz, 1 Pa). $T_{sol\text{-}gel}$ was defined as the temperature at which the material transitioned from a predominantly viscous state ($G'' > G'$) to a predominantly elastic state ($G' > G''$) [31].

For the mucoadhesive investigation, an appropriate amount of mucin powder (10% *w*/w) was dispersed in Milli-Q water or directly in the copolymeric "solutions". Firstly, viscosity measurements were conducted at 37 °C using a rotational rheometer over a shear rate range of 0.1 to 100 s^{-1}, as previously described. The apparent viscosity values recorded at selected shear rates (25, 50, 75, and 100 s^{-1}) were subsequently used to calculate the Mucoadhesion Index (Δη), also referred to as "rheological synergism", according to the following equation:

$$\Delta\eta = \eta_{mix} - (\eta_{hydrogel} + \eta_{mucin})$$

where η_{mix}, $\eta_{hydrogel}$, and η_{mucin} represent the apparent viscosities (Pa·s) of the mixture of thermosensitive vehicles and mucin dispersion, the P407-based hydrogels, and the mucin dispersion, respectively [30,32].

For a mucoadhesive formulation, η_{mix} is higher than $\eta_{hydrogel} + \eta_{mucin}$ due to the interaction occurring between the polymeric system and mucin, resulting in positive Δη values [33,34].

Additionally, a frequency sweep test on the mucin/hydrogel mixtures was carried out in order to investigate the potential nature of the interactions between the P407-based formulations and the glycoprotein [32,35].

2.2.3. In vitro dissolution and drug release studies

The release profile of 5-ASA from the thermo-responsive systems was evaluated at pH 5.0 and 7.4 by both the dialysis method and a membrane-less procedure, investigating at the same time the dissolution rate of the formulations [36,37]. One gram of the copolymer solution was transferred into pre-weighed 3 mL glass vials and incubated at 37 °C until a clear gel was formed. Following complete gelation, 2 mL of 10 mM PBS were carefully layered over each hydrogel. At predetermined time intervals, the release medium was removed, the vials were reweighed and fresh PBS was added. Gel dissolution was quantified by calculating the difference in vial weight before and after incubation, with results expressed as a percentage [36,37]. All samples were maintained at 37 °C throughout the duration of the study.

Release of the bioactive was obtained by analyzing aliquots of the release medium using a spectrophotometric method (PerkinElmer Lambda 35 UV–vis spectrophotometer, GmbH Uberlingen, Germany), as previously described [38].

The release of the bioactive was also investigated by the dialysis method. Specifically, 5 g of each formulation were placed into dialysis bags (cellulose acetate, molecular weight cut-off 3500 Da; Spectrum Laboratories Inc., Netherlands), sealed at both ends and immersed in 100 mL of phosphate-buffered saline (PBS) under continuous stirring to maintain sink conditions. At predetermined time intervals, 1 mL of the release medium was withdrawn and replaced with an equal volume of fresh PBS. The collected samples were successively analyzed using a UV–vis spectrophotometer [24].

The release kinetics was investigated applying various mathematical models, including zero-order, first-order, Higuchi, Korsmeyer-Peppas and Hixson-Crowell. The model with the highest correlation coefficient (R^2) was considered the most suitable for accurately describing the mechanism of drug leakage [38,39].

2.2.4. Gelation time and gel strength

The gelation time at room temperature (25 ± 2 °C) was assessed using the test tube inversion method. [40] Briefly, the formulation in the liquid state was transferred into a vial and heated in a water bath. At predetermined time intervals, the vial was removed and inverted to check for gel formation. The time was recorded using a stopwatch, which was paused whenever the vial was taken out of the water bath. The gelation time was defined as the point when the sample no longer flowed upon inversion [41].

Gel strength was evaluated following the method described by Firoz and colleagues, by transferring the sample into a graduated cylinder and allowing it to gel at 37 ± 1 °C. [42] After gelation, weights were applied onto the gelled sample, and the time required for it to sink 5 cm into the formulation was recorded. If the apparatus required more than 300 s to descend, additional weights were incrementally added. Gel strength was determined based on the minimum weight necessary to displace the apparatus by 5 cm through the copolymeric matrix [42,43].

2.2.5. Injectability and spreadability tests

The injectability of the thermo-sensitive systems was assessed at room temperature. The formulation, containing 0.25% (w/w) 5-ASA, was loaded as liquid form into a needleless syringe fitted with a Luer slip tip (inner diameter: 4 mm) to simulate the cannula of a microenema and subsequently injected into PBS preheated to 37 °C [42].

To evaluate the spreadability of the hydrogels, a 0.1 g of sample was placed at the center of a glass plate and covered with a second glass plate of identical dimensions. A 50 g weight was gently applied on top to facilitate the spreading of the gel between the plates. After 5 min, the weight was removed, and the diameter (in cm) of the spread area was measured. The test was performed in triplicate [26,42].

2.2.6. FT-IR analysis and DPPH radical scavenging assay

The FT-IR spectra of freeze-dried hydrogels either as blank formulations or containing 5-ASA and the single components (P407, 5-ASA) were evaluated by a Nicolet iS5 spectrometer equipped with an iD7 attenuated total reflectance accessory (Thermo Fisher Scientific Inc., Waltham, MA, USA), as previously reported [44].

Spectra data were processed using OMNIC software, version 9.12.1019. The results presented are a representative analysis of three independent experiments.

The antioxidant capacity of the different components and formulations was assessed using the DPPH assay [45]. A 5-ASA (10, 25, and 50 μg/mL) was solubilized in ethanol. Successively, 100 μL of an ethanol solution of DPPH (0.1 mM) were combined with 100 μL of the samples in a 96-well microplate and incubated for 30 min at room temperature in the dark. Following incubation, the absorbance was recorded at 517 nm

using a microplate reader (Varioskan LUX; Thermo Fisher Scientific, Milan, Italy).

The percentage of DPPH radical inhibition was determined using the following equation:

$$\text{DPPH inhibition } (\%) = \left(1 - A_{sample}/A_{control}\right) \times 100$$

where A_{sample} represents the absorbance of the test sample and $A_{control}$ corresponds to the absorbance of the control (DPPH solution without sample). The solvent used as a blank was included in each measurement to correct for background absorbance [45].

2.3. Preclinical characterization in cell and murine IBD models of the anti-inflammatory properties of P407-5-ASA

2.3.1. Cell lines and culture conditions

The human colon epithelial cell line Caco-2 were gifted by Dr. Palumbo (Institute of Biostructures and Bioimaging, CNR), murine macrophages RAW 264.7 and human fibroblasts were purchased from the American Type Culture Collection (ATCC, Manassas, VA, USA). All cell lines were grown in Dulbecco's modified Eagle's medium (DMEM) supplemented with 10% Fetal Bovine Serum (FBS), 1% penicillin-streptomycin and 1% L-Glutamine in a humidified incubator at 37 °C and 5% CO_2 [46].

2.3.2. Inflammation of RAW264.7 macrophages by lipopolysaccharide (LPS)

RAW264.7 macrophages were activated by the bacterial antigen lipopolysaccharide, LPS (lipopolysaccharide from *E. coli*, Sigma Aldrich, Merck Millipore, USA). In details, $3{\cdot}10^5$ cells were seeded in 6 well-plates and exposed to 200 ng/mL of LPS in serum-free culture medium for 24 h. Polarization to M1 pro-inflammatory phenotype was evaluated by morphological analysis of the development of foam-cells like phenotype using Eclipse Ti2 inverted microscope (Nikon Instruments Inc., Melville, NY, USA), and by western blot analysis of the expression levels of pro-inflammatory markers such as inducible nitric oxide synthase (iNOS), and p-ERK/ERK ratio. Western Blotting was performed as previously described [47]. Briefly, cells were lysed using a lysis buffer containing 40 mM HEPES (pH 7.5), 120 mM NaCl, 5 mM $MgCl_2$, 1 mM EGTA, 0.5 mM EDTA and 1% Triton X-100, supplemented with phosphatase inhibitors (20 mM α-glycerol-3-phosphate and 2.5 mM sodium pyrophosphate) and protease inhibitors (Complete Tablets, EDTA-free, Roche). Following lysis, the cell lysates were centrifuged at 13,200 RPM for 20 min at 4 °C. Protein concentrations were determined using the Bradford assay (Bio-Rad, Protein Assay). Equal amounts of protein were then separated on 4–12% SDS-PAGE gels and transferred to nitrocellulose membranes. Membranes were blocked for 1 h with 5% non-fat dry milk and subsequently incubated overnight with primary antibodies targeting: iNOS (A14031, ABclonal), ERK (CST 9102), phospho-ERK (CST 9101) and α-Tubulin (sc-528). After washing with PBS containing 0.1% Tween-20, membranes were incubated with appropriate secondary antibodies for 1 h and visualized using the enhanced chemiluminescence (ECL) detection system [48].

2.3.3. Evaluation of anti-inflammatory properties of P407 and P407-5-ASA on Caco-2 cells

Caco-2 cells ($2{\cdot}10^5$, 12 well plate) were seeded in the basolateral compartment of a Boyden chamber (8 μm insert, previously coated with PBS-diluted Matrigel in a 1:5 Matrigel/PBS ratio) and treated with free 5-ASA (5 mM), P407 and P407-5-ASA (5 mM of drug); P407 dose was the same for all treatments. The formation of a functional tight junction monolayer by Caco-2 cells was assessed by measuring transepithelial electrical resistance (TEER) using a Millicell ERS voltmeter [49,50]. Cells were cultured until a stable epithelial barrier was achieved, as indicated by TEER values exceeding 500 $\Omega{\cdot}cm^2$ [49,50]. RAW 264.7 M1 macrophages (10^5 cells, in serum free DMEM and in presence or absence of LPS 200 ng/mL) were seeded in the upper chamber and co-cultured with Caco-2 for 48 h. After co-culture, RAW 264.7 M1 macrophages were stained with crystal violet (30 min incubation at 4 °C). The excess staining solution was meticulously removed from the inserts by three thorough water washes. Following the removal of non-invading cells by means of a cotton-swab, the number of invading macrophages was evaluated in at least five different spots of the insert under a phase contrast microscope (Eclipse Ti2-Nikon inverted microscope, 10× magnification) [51]. The inflammatory cytokine TNF-α released by RAW 264.7 M1 macrophages in culture medium at the end of the co-culture procedure was evaluated by ELISA (Pro: Mouse TNF-α, 3511-1HP-1, Mabtech, Italy). The results are reported as the mean ± standard deviation of at least three independent experiments.

As a preliminary safety assessment, the cytotoxicity of the different formulations was evaluated after 24 h incubation with human fibroblasts using the 3-(4,5-dimethylthiazol-2-yl)-2,5-diphenyltetrazolium bromide (MTT) assay [52]. The cells were employed as a representative non-transformed cell line in order to preliminarily assess the cytocompatibility before proceeding with the *in vitro* experiments on Caco-2 cells. Untreated cells were used as the control.

2.3.4. Caco-2 cell differentiation in intestinal enterocytes (iECs)

Caco-2 cells differentiation in intestinal enterocytes (iECs) was performed with an adapted protocol as previously described [53]. Briefly, iECs were obtained by seeding Caco-2 cells at a density of $3{\cdot}10^4$ cells/cm^2 and growing them in DMEM supplemented with 20% FBS, 1% penicillin-streptomycin and 1% L-Glutamine in a humidified incubator at 37 °C, 5% CO_2 for 14–21 days, replacing the medium every other day. Cell differentiation was followed over time by live imaging (Nikon Eclipse Ti2 inverted microscope). *Z*-stack acquisitions (step-size 0.5 μm, up to 80 μm thickness) were performed to assess the presence of domes and the development of villi by 3D reconstruction using the NIS-elements AR software.

2.3.5. Inflammation of intestinal enterocytes (iECs) derived by Caco-2 cells

iECs obtained as above described were inflamed by exposure to LPS (200 ng/mL) or conditioned medium from LPS-inflamed RAW 264.7 for 24 h. Differentiated monolayers were characterized for the characteristic inter-villi distance by ImageJ software (v.1.54 g) and its alteration in differently treated monolayers was used as quantitative indication of the pro-inflammatory treatment effects on the structural integrity of the monolayer.

2.3.6. Evaluation of anti-inflammatory effect of P407 and P407-5-ASA in an optimized in vitro model of intestinal inflammation

Co-culture of differentiated Caco-2 cells in iECs and LPS-inflamed RAW 264-7 macrophages was used as an optimized *in vitro* testing platform for further evaluation of the anti-inflammatory effect of the developed hydrogel formulation. The migration of M1 macrophages towards iECs treated with free 5-ASA (5 mM), P407 and P407-5-ASA (5 mM of drug) was evaluated in Boyden chamber (3 μm insert, 6 well plate) where iECs stayed in the basolateral compartment while LPS-inflamed and Vivotrack 680 stained RAW 264.7 ($3{\cdot}10^5$cells/insert) were seeded in the upper chamber [48]. After 24 h, fluorescent imaging of both the apical and the basolateral compartments of the chamber by Nikon Eclipse Ti2 inverted microscope allowed to visualize and quantify the infiltration of M1 macrophages in the epithelium.

2.3.7. Mucoadhesive properties and therapeutic efficacy of P407-5-ASA in an IBD murine model

All experimental procedures complied with the European Communities Council directives (2010/63/EU) and the present study was approved by the Italian Ministry of Health (authorization number 1133/2024-PR).

To minimize animal suffering all the experimental procedures described were performed under general anesthesia with 1.5%

isoflurane in 100% oxygen at 0.8 L/min. Mice were maintained on a diet with a purified, alfalfa-free rodent chow for 15 days before fluorescence imaging to minimize fluorescence in the gut.

The colitis model was established in CD1 female mice treated with 3% low molecular weight dextran sodium sulfate salt (DSS, 42867, Sigma-Aldrich) in drinking water for 10 days and the disease progression was evaluated daily by monitoring mice body weight, stool consistency and the presence of rectal bleeding. A score was associated with each of these parameters and their composition was used to quantitatively estimate the pathology progression by the Disease Activity Index (DAI) [54].

The colon-adhesive *in vivo* property of P407-based formulation was evaluated in CD1 mice by molecular imaging using high-frequency ultrasound-guided (HFSU, VEVO 2100, FUJIFILM VisualSonics, Inc., Toronto, 270 Ontario, Canada) [55], rectal administration of 50 μL of rhodamine-loaded hydrogel that allowed to precisely evaluate its deposition whereas its colon-retention over time was assessed by *ex vivo* fluorescent imaging of excised colons at 3 and 24 hour post administration (Vilber Newton 7.0 FT-500 system $\lambda_{ex/em}$ = 542/570 nm).

To evaluate the therapeutic efficacy of the anti-inflammatory thermo-sensitive formulations mice were divided into two groups: one group of healthy mice ($n = 4$) that drank water and one group of colitis-bearing mice receiving 3% DSS in drinking water ($n = 12$). On the 10th day of DSS treatment, colitis-bearing mice were randomized in four groups as follows: untreated ($n = 3$), ASAMAX (n = 3), P407 (n = 3), P470-ASA (n = 3) and treated daily for 5 days with treatments consisting of rectal administration of 50 μL of ASAMAX in Vaseline oil (16 mM of 5-ASA), P407 or P407-5ASA (16 mM of 5-ASA), respectively. At the end of the treatment, DAI was evaluated, and animals were euthanized. Colon and spleen length were measured by a ruler, and spleens were weighed to estimate inflammation [54].

2.4. Statistical analysis

Statistical analysis of the various experiments was performed by One-way ANOVA or Student's *t*-test with a p value <0.05 considered statistically significant.

3. Results and discussion

3.1. Preparation and characterization of 5-ASA-loaded P407 hydrogels

5-ASA is widely used as a first-line treatment for IBD, especially ulcerative colitis, but its oral bioavailability is limited by poor water solubility and enzymatic degradation in the upper GI tract; rectal administration using P407-based thermo-sensitive hydrogels offers a promising alternative by bypassing the upper GI tract, achieving high local drug concentrations and minimizing the potential systemic side effects. P407 concentrations between 15 and 25% w/w ensure a sol-gel transition close to 37 °C, enabling easy administration, *in situ* gelation, prolonged mucosal contact and sustained release of poorly water-soluble bioactives such as 5-ASA, without the need of organic solvents that could cause adverse effects, particularly on colonic mucosa already compromised by IBD.

In this work, P407-based hydrogels (20% *w*/w) containing various amounts of 5-ASA were developed in order to evaluate the saturation limit of the poloxamer system (Table 1). 5-ASA was incorporated as powder form at concentrations up to 0.25% w/w; increasing the amount of the active compound up to 0.5% w/w promoted a visible drug precipitation (Fig. S1).

Table 1
Composition and gelation temperature of various *in situ* rectal gel formulations.

Formulation	5-ASA (% w/w)	$T_{sol\text{-}gel}$ (°C)
Blank	–	24.10
F1	0.10	24.04
F2	0.25	23.25
F3	0.30	Drug precipitation
F4	0.50	Drug precipitation

3.1.1. Rheological analysis

Rheological analysis is essential for the characterization of thermo-sensitive hydrogels proposed for rectal delivery of active compounds. Key parameters such as viscosity, gelation temperature and viscoelastic properties (G′ and G″) influence the injectability of a formulation at room temperature and its properties of gelling and be retained in a specific body compartment at body temperature. The refinement of these characteristics ensures effective mucosal adhesion, sustained drug release and patient comfort. Rheology also simulates administration conditions, helping to predict the *in vivo* fate of a system [56].

The thermo-sensitive behavior of P407 systems and the effect of 5-ASA were assessed using passive microrheology, which analyzes viscoelastic properties without external forces. Samples stored at 4 °C were transferred to a 37 °C environment to simulate physiological conditions. Initially, high MSD values indicated a fluid state characterized by a high mobility of particles (Fig. 1A). Over 30 min, MSD values decreased, reflecting the sol-gel transition and hydrogel network formation driven by temperature-induced micellization of P407 into packed micelles forming a physical gel [57].

MSD curves, serving as the viscoelastic fingerprint of the formulations, enabled the derivation of parameters such as SLB and EI (Fig. 1B and C). The results confirmed that the presence of the bioactive at the tested concentration did not affect the thermo-sensitive behavior of the P407-based systems. Initial SLB values above 0.5 indicated a liquid-like state, while values approaching 0 at 37 °C demonstrated a transition to a solid-like phase (Fig. 1B) [44].

Moreover, EI data show that the presence of 5-ASA leads to a slight, proportional increase in elasticity with increasing drug concentration (Fig. 1C).

This trend was further confirmed by dynamic rheology tests. All systems showed a Newtonian behavior with constant viscosity at low temperature (10 °C), and transitioned to a non-Newtonian, shear-thinning profile at 37 °C, where viscosity (η) decreased when the shear rate (γ) increased (Fig. 2A) [17]. 5-ASA induced a slight increase of viscosity compared to the drug-free hydrogel, without altering the peculiar shear-thinning behavior of the systems. This property is particularly advantageous for rectal administration because it facilitates the application, enhances patient compliance and promotes the potential retention rate of the formulation (Fig. 2A) [58,59].

Oscillatory tests were performed to evaluate the viscoelastic properties of the hydrogels. [17] An amplitude sweep (0.1–100 Pa) confirmed a well-defined LVR, with both G′ and G″ remaining constant throughout the range (Fig. 2B). Based on these results, a shear stress of 1 Pa was selected for the frequency and temperature sweep measurements [28].

The frequency sweep test is a crucial rheological analysis for hydrogels intended for rectal drug administration, as it provides insight into their viscoelastic behavior under physiological conditions. This test is useful to investigate the structural stability and mechanical strength of the system by evaluating the storage (G′) and loss (G″) moduli over a range of angular frequencies [60]. As shown in the Fig. 2C, G′ was significantly greater than G″ across the whole frequency range tested at 37 °C, indicating that the elastic component is predominant and that the sample exhibited typical gel-like behavior, essential for an adequate retention at the site of application [59].

The $T_{sol\text{-}gel}$ of the liquid suppositories was determined by monitoring changes in the elastic (G′) and viscous (G″) moduli over a temperature range of 10 to 40 °C. $T_{sol\text{-}gel}$ was defined as the temperature at which G′ and G″ intersect, marking the transition from predominantly viscous behavior (G″ > G′) to predominantly elastic behavior (G′ > G″) (Fig. S2) [31]. As shown in Fig. 2D, the $T_{sol\text{-}gel}$ value of the drug-free formulation

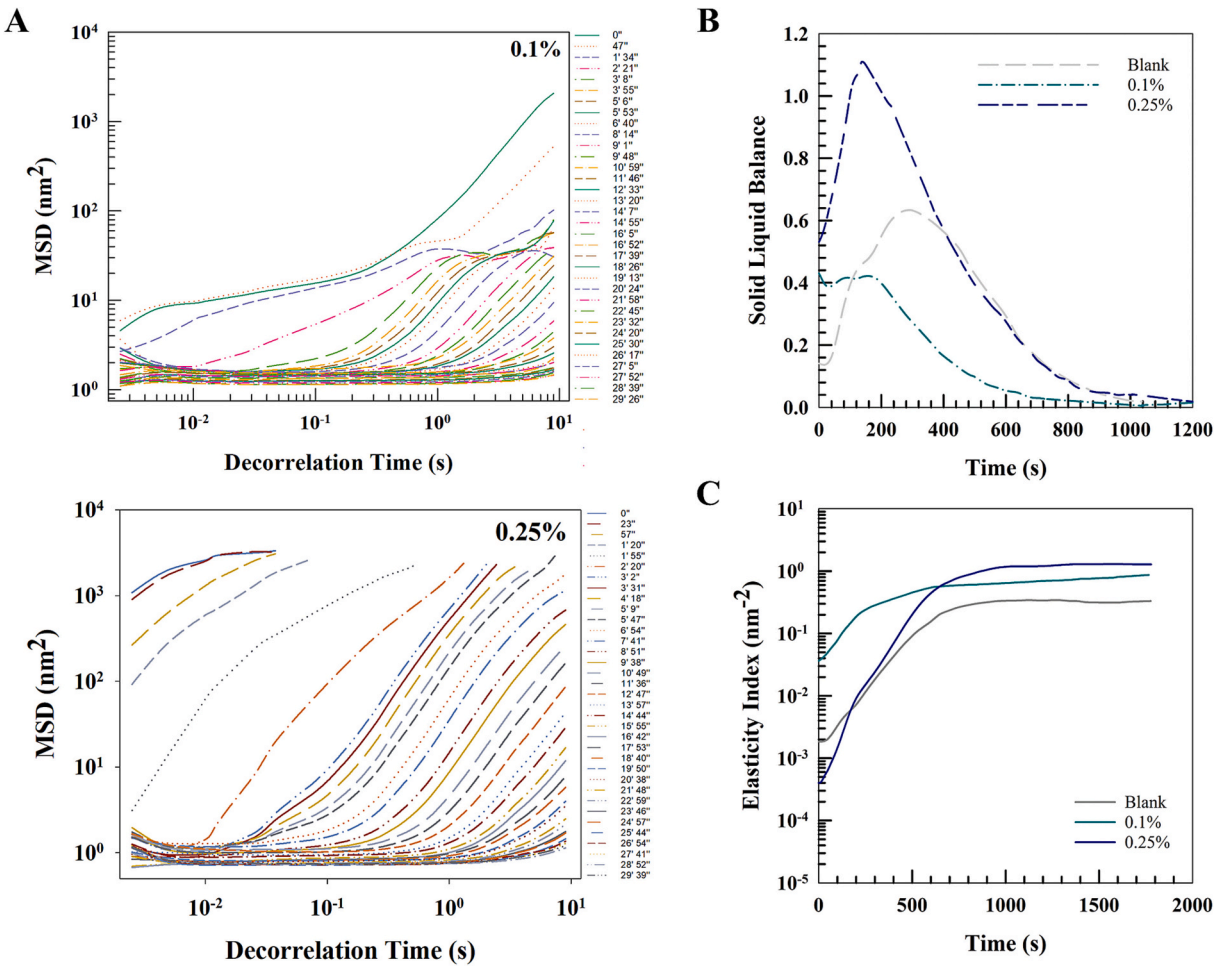

Fig. 1. Mean square displacement (MSD) curves (A), solid-liquid balance profiles (B) and elasticity index (C) of 5-ASA-loaded P407 hydrogels as a function of the drug concentration and decorrelation time.

was 24 °C, consistent with values typically reported for P407-based hydrogels prepared with 20% *w*/w of the copolymer, as also demonstrated by our research team [24,61].

The addition of 5-ASA slightly decreased the $T_{sol\text{-}gel}$ of the formulation, from 24.10 °C to 23.25 °C at the highest concentration tested, while it remained almost constant when 0.1% w/w of drug was employed (Fig. 2D). This temperature shift, along with the slight increase in viscosity, suggests an enhanced intermicellar association, likely driven by hydrophobic interactions between 5-ASA and the POP residues of P407. These results are in agreement with other experimental formulations focused on the characterization of P407 containing poorly water-soluble drugs [26].

Although a $T_{sol\text{-}gel}$ of 30–35 °C is usually required for a thermosensitive system proposed for rectal administration [62], a slightly lower $T_{sol\text{-}gel}$ can be advantageous for formulations designed to rapidly gel upon contact with body temperature. In this context, a $T_{sol\text{-}gel}$ of ~24 °C ensures immediate gel formation after rectal administration, thereby limiting formulation leakage and promoting early mucosal retention. It is well established that, in P407-based systems, the $T_{sol\text{-}gel}$ is inversely related to copolymer concentration, with higher polymer contents leading to lower $T_{sol\text{-}gel}$ values [18]. The use of a lower copolymer concentration to achieve higher transition temperature may result in a formulation with lower viscosity and weaker gel strength, which could compromise its suitability for rectal administration, whereas higher copolymer concentrations may promote a rapid gelation at room temperature, compromising the handling feasibility during formulation preparation and administration [22,43,57]. Therefore, the formulation design requires a careful balance between achieving sufficiently rapid *in situ* gelation after administration and avoiding premature gelation during handling or inadequate mechanical strength at lower copolymer concentrations. The selected P407 concentration therefore represents a suitable parameter, ensuring adequate mechanical strength and mucosal retention while preserving appropriate handling characteristics before the administration. To further address this aspect, a phase of characterization was focused on the evaluation of the gelation time of the formulation at room temperature, to be studied for a conceivable administration as a liquid form, with respect to that at body temperature (37 °C) (Section 3.1.3).

Mucoadhesion represents another critical parameter in the development of pharmaceutical formulations for rectal drug delivery. The term refers to the interaction between a system and the mucous layers [63,64]. An increase of adhesion to the mucosa prolongs the residence time of the drug in the rectum, promoting an enhanced overall bioavailability [22].

Rheological analysis is a widely used approach to assess the mucoadhesive potential of a pharmaceutical formulation. Typically, mucoadhesive systems demonstrate a rheological response in mucin-formulation mixtures that exceeds the sum of the individual responses, a phenomenon known as "rheological synergism" [32,34].

Fig. 2E shows the variation of the mucoadhesion index ($\Delta\eta$) with respect to shear rate. Positive $\Delta\eta$ values were obtained at all tested shear rates, demonstrating the mucoadhesive properties of the P407 hydrogels containing mesalazine. The POE component contributes to these properties through its capacity to form interactions with the oligosaccharide

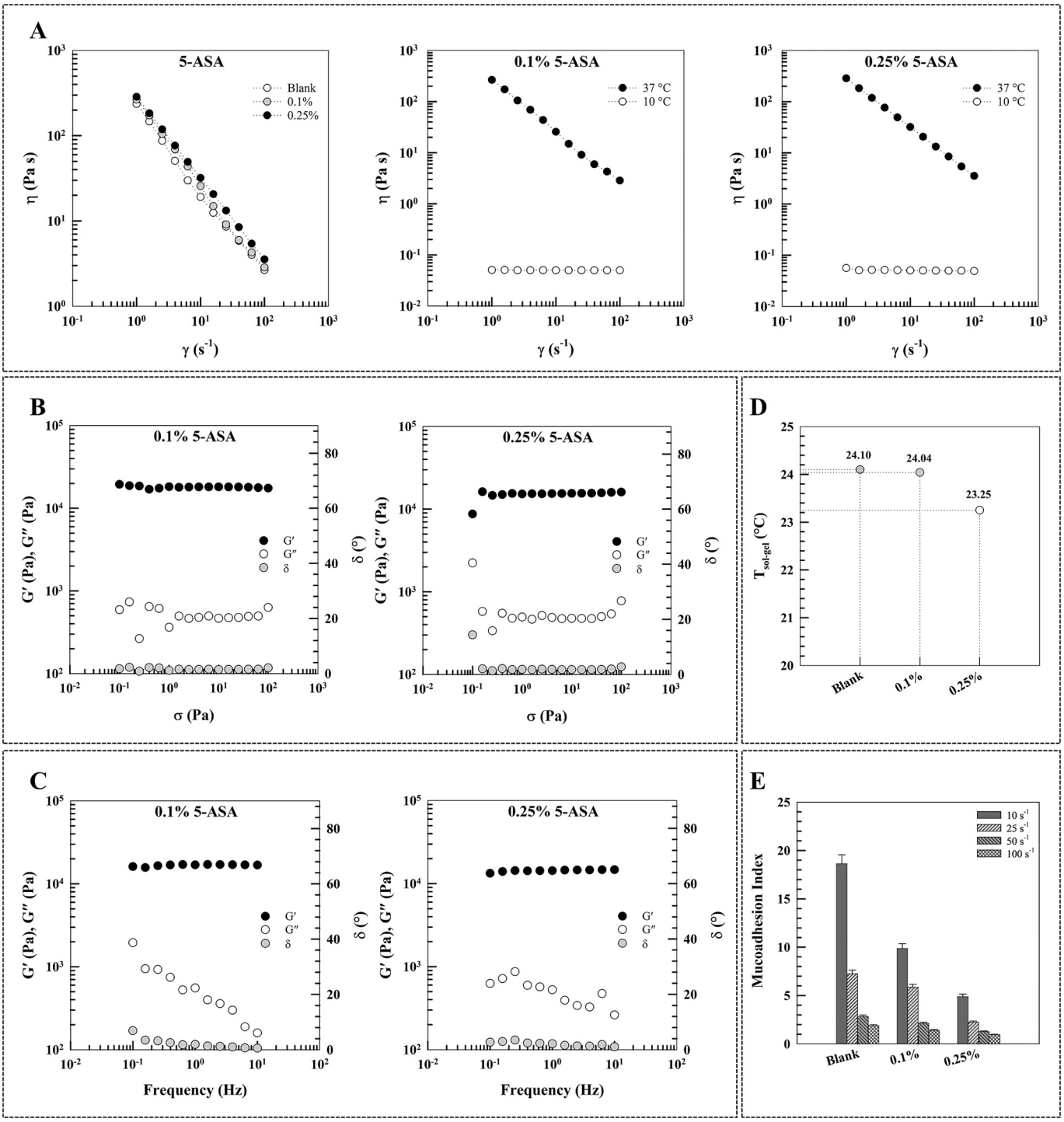

Fig. 2. Shear rate viscosity of P407 (20%, w/w) hydrogels containing 5-ASA (A). Elastic modulus (G′), viscous modulus (G″) and phase angle (δ) of 5-ASA-loaded P407 hydrogels as a function of shear stress (B) and frequency (C). The analyses were performed at 37 °C. Sol-gel transition temperature ($T_{sol\text{-}gel}$) of the P407-based formulations (D). Mucoadhesion index values of 5-ASA (0–0.25% w/w)-loaded P407 hydrogels measured at 37 °C as a function of the shear rate (10, 25, 50, and 100 s^{-1}) (E).

chains of mucin, supporting its application as a biomaterial for rectal drug delivery [65].

The presence of the drug caused a slight reduction in the mucoadhesion index; however, the obtained values remained positive. This observation is consistent with previous reports indicating that the incorporation of additional polymers or active compounds can influence the bioadhesive and mucoadhesive properties of P407 [22]. The use of supplementary materials to enhance the mucoadhesiveness of poloxamer-based systems remains a topic under investigation and it of debate by the scientific community [66,67]. While such strategies may improve adhesion, excessive mucoadhesion can compromise rectal mucosa integrity, and the addition of bioadhesive agents to poloxamer-based liquid suppositories may increase the risk of tissue irritation [22]. The findings of this study further supported by the *in vivo* results (Section 3.2.3) demonstrate that the formulation, even without additional polymers, is capable of extending the residence time of 5-ASA in the bowel

compartment. This offers a promising approach that avoids unnecessary costs and minimizes the potential adverse effects exerted by additional components.

Oscillatory rheological tests were performed over a frequency range of 0.1–10 Hz to investigate the potential nature of the interactions between P407 formulations and mucin. Depending on the interaction type, three mechanical behaviors may be observed: (i) G′ significantly greater than G″, demonstrating a chemical cross-linking; (ii) G′ slightly greater than G″, suggesting interactions *via* secondary bonds and (iii) G′ equal to or less than G″, typical of physical cross-linking [30]. The mechanical spectra of the various formulations showed a dominant storage modulus (G′ > G″), suggesting the establishment of chemical interactions between the copolymer and mucin (Figs. 2 and S3).

3.1.2. *In vitro* dissolution behavior and drug release kinetics

The dissolution and drug release behavior of P407-based hydrogels are key factors to be investigated during the characterization of a formulation proposed for rectal application because they directly influence the retention rate of an active compound at the administration compartment and its availability at the site of inflammation. These properties are essential to ensure the therapeutic efficacy of a formulation proposed for the treatment of IBD and to improve the patient compliance [24,68].

The dissolution profiles of the developed formulations are shown in Fig. 3A. P407-based hydrogels showed a rapid and complete dissolution in aqueous media after 24 h, a behavior attributed to the high solubility in water of the copolymer and in agreement with other experimental investigations [69]. The presence of 5-ASA at the tested concentrations did not significantly affect the dissolution rate of the thermo-sensitive P407-based systems (Fig. 3A).

The *in vitro* release profile of the 5-ASA from P407-based hydrogels was evaluated under physiological conditions in PBS at 37 °C (Fig. 3B). Two complementary approaches were employed to better simulate different release conditions: the membraneless diffusion and the dialysis setup [40]. In the dialysis method, the hydrogel was physically separated from the release medium, thereby limiting copolymer dissolution and resulting in a release profile primarily governed by diffusion. On the contrary, the membraneless method allowed a direct contact between the gel and the surrounding medium, facilitating the dissolution of the polymeric matrix. As reported in the literature, drug release from hydrogels generally involves a combination of both diffusion and dissolution mechanisms [70,71].

As shown in Fig. 3B, using the membraneless method, the release of the anti-inflammatory drug from P407 hydrogels reached approximately 40% and 60% after 24 h for formulations containing 0.1% *w*/w and 0.25% w/w of 5-ASA, respectively. Conversely, with the dialysis method, the drug release was sustained over a 48-hour period for all tested formulations, with an initial burst release observed during the first 8 h, data consistent with those of dissolution previously described in Fig. 3A.

The release mechanism of 5-ASA from the thermo-sensitive system can be described in two phases: an initial burst release driven by hydrogel dissolution and the rapid release of unentrapped drug, followed by a sustained leakage of 5-ASA in which the active compound gradually diffuses from the P407 micellar network [72]. This behavior can be explained by considering the thermo-responsive micellization

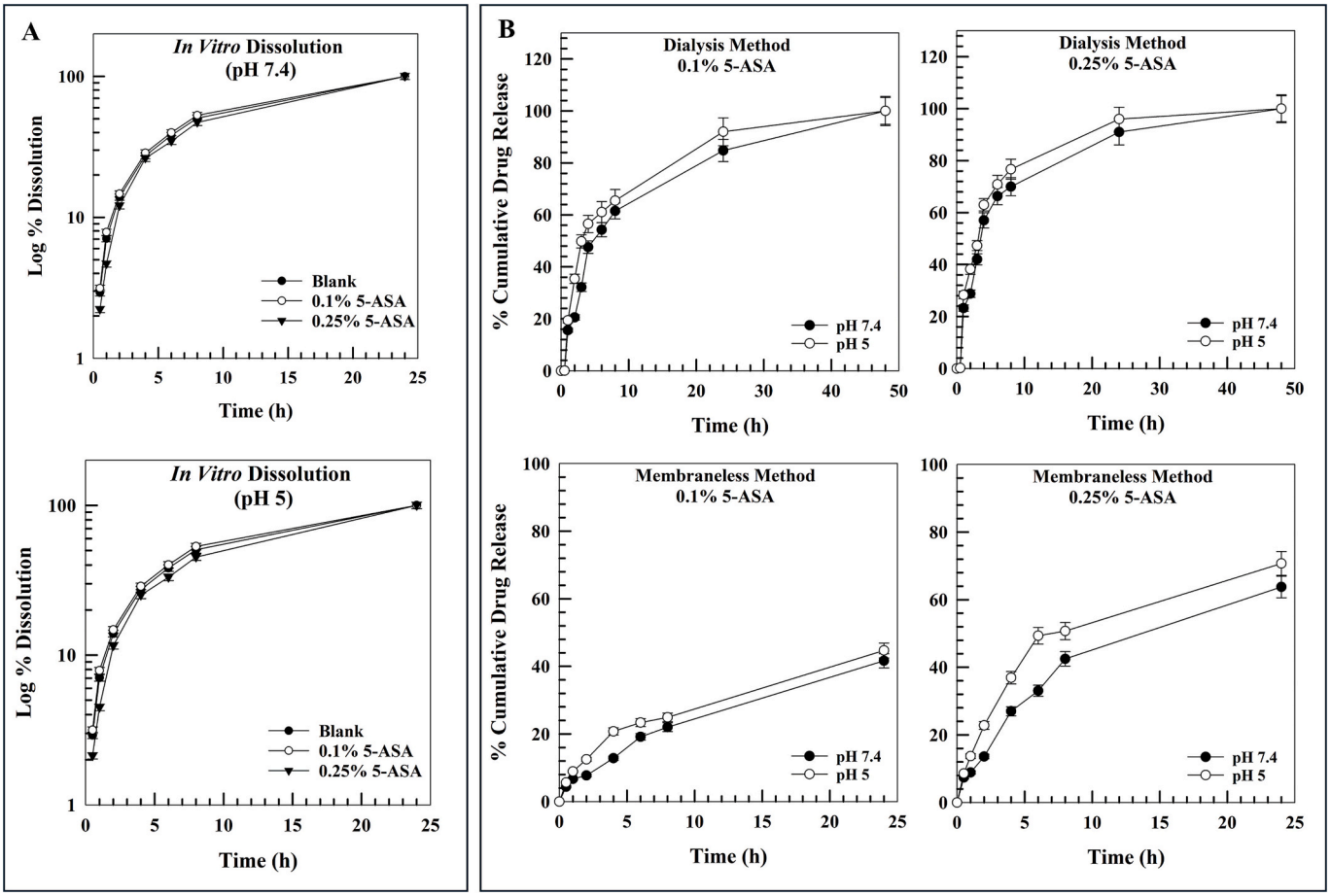

Fig. 3. Dissolution profiles of P407-based hydrogels at 37 °C in phosphate-buffered solution (pH 7.4) and at pH 5. Data were expressed as percentage of weight loss (% w/w) as a function of time (A). *In vitro* cumulative drug release of P407-based hydrogels at 37 °C in phosphate-buffered solution (pH 7.4) and at pH 5. Release studies were performed using the dialysis method (B) and the membraneless method (C).

and gelation properties of P407. P407 is an amphiphilic triblock copolymer whose behavior is governed by its critical micellization concentration (CMC) and critical micellization temperature (CMT) [73]. At the copolymer concentration employed in this study and at physiological temperature, both the CMC and CMT are exceeded, promoting the spontaneous self-assembly of P407 molecules into micelles characterized by a hydrophobic POP core and a hydrophilic POE shell [24].

When the temperature increases, dehydration of the POE chains and enhanced hydrophobic interactions among POP blocks drive micelle formation and their close packing into a three-dimensional network, ultimately leading to the sol-gel transition. This micellar network provides a suitable environment for the incorporation of poorly water-soluble compounds such as 5-ASA, which preferentially partition into the hydrophobic core of micelles, as confirmed by FT-IR analysis (Section 3.1.5) [24,27].

Accordingly, the initial burst release is mainly attributed to the rapid diffusion of drug molecules located at or close to the hydrogel surface or weakly associated with the polymeric matrix, as well as to early-stage hydrogel relaxation and partial dissolution. This phase is followed by a sustained release phase governed by the diffusion of 5-ASA from the micellar core through the hydrated gel network, together with the gradual dissolution of the P407 matrix over time.

The obtained results support the potential application of 5-ASA-loaded P407 hydrogels for rectal application because they can potentially enhance the therapeutic outcome of the active compound. Namely, the initial burst release can ensure a rapid achievement of therapeutic levels, while the micellar structure can promote a prolonged drug release over the time, decreasing the administration times.

As is well known, the gastrointestinal tract (GIT) possesses various pH across different regions. The stomach is characterized by an acidic environment, while the small intestine has a slightly acidic to neutral pH. The pH of colon and rectum typically ranges from 6.1 to 7.5 [74].

However, gastrointestinal pH can be altered in IBD, sometimes reaching pH 5, which can influence the efficacy of therapeutic formulations. These alterations result from several physiological and pathological processes, including mucosal bicarbonate secretion, microbial lactate production, impaired absorption of short-chain fatty acids, and changes in intestinal fluid volume, carbohydrate metabolism, and gastrointestinal transit time [74]. For this reason, drug dissolution and release tests were also performed at pH 5) in order to better mimic the altered physiological conditions associated with IBD.

Indeed, it is well-known that the behavior of P407-based hydrogels can be affected by the presence of drugs, polymers, salts or pH variation [18,22].

The release of 5-ASA at pH 5 was slightly faster than that obtained at pH 7.4 (Fig. 3), probably as a consequence of the presence of HCl able to decrease the strength of P407 hydrogels [75]. This phenomenon leads to a greater dissolution in aqueous media of the gel matrix and, consequently, to an increased drug release over time. However, the observed differences were minimal, confirming that the P407 hydrogel remains a suitable system for rectal administration of 5-ASA.

The release data were fitted according to zero-order, first-order, Higuchi, Korsmeyer-Peppas and Hixson-Crowell kinetic models (Tables S1 and S2).

The results demonstrate that the Higuchi model best describes the *in vitro* release profile of 5-ASA when the membraneless method is applied. This model reflects a diffusion-controlled release mechanism, in which the drug diffuses through channels within the hydrogel matrix. On the contrary, first-order kinetics were characteristics of the release behavior observed when the dialysis membrane method was employed, showing that the bioactive is dispersed inside the porous matrices and the rate of drug release was concentration-dependent over time [26,39,62].

3.1.3. Gelation time and gel strength determination

Liquid suppository systems are specifically designed to remain in a liquid state at room temperature and undergo gelation at body temperature [62]. For this reason, the $T_{sol\text{-}gel}$ should ideally fall within the range of 33–37 °C to minimize complications related to manufacturing, storage, and potential post-administration leakage [76].

As previously reported, P407-based formulations containing 5-ASA (0.25% w/w) showed a $T_{sol\text{-}gel}$ below 25 °C (Section 3.1.2), which could be an issue during the sample administration at room temperature. Consequently, the next phase of the study focused on the evaluation of the gelation time of the proposed formulations. The system prepared with the highest concentration of 5-ASA was selected for the test. When placed in a 25 ± 2 °C water bath, the P407 solution transitioned into a gel status after approximately 6 min, remaining stationary at the bottom of the inverted vial (Fig. S4 and Video S1) [77]. This time frame is suitable for a suitable administration of a liquid suppository at room temperature.

Gel strength is another key parameter to be evaluated because it influences the ease of application of as suppository and it helps to prevent the anal leakage [78]. In fact, while high gel strength may hinder the administration, a low gel strength can result in rectal leakage, reducing the retention rate of the formulation and the therapeutic effectiveness [78]. Previous studies have shown that ideal *in situ* rectal gels should exhibit gel strength values in the range of 10–50 s [42,79].

In this context, Choi et al. developed mucoadhesive liquid suppositories based on poloxamers for rectal delivery of acetaminophen and investigated the relationship between formulation composition, gel strength and *in vivo* performance [80]. The formulations made up of P407, poloxamer P188 and various concentrations of the bioadhesive polymer polycarbophil were designed to achieve an *in situ* gelation at body temperature, enhancing the rectal retention and drug bioavailability. The authors demonstrated that formulations characterized by low gel strength (~9 s) were unable to remain *in situ* after rectal administration and they showed a marked leakage after their injection, as evidenced by the need to seal the anus during pharmacokinetic experiments. On the contrary, the formulations characterized by higher gel strength values (~34 s) formed strongly gelled and mucoadhesive systems that remained localized within the rectum without leakage, promoting a sustained drug release, prolonged plasma exposure and an enhanced bioavailability of the active compound [80].

The formulation herein described was characterized by a gel strength exceeding 300 s, which is above the minimum range value required of 10–15 s (Video S2 and Fig. S5) [42,79]. This result confirms that the formulation possesses a robust gel structure capable of maintaining the gel-like properties over time, as previously demonstrated through oscillatory rheological measurements (Section 3.1.1). Moreover, these *in vitro* findings were further validated by *in vivo* studies performed on mice, as described in the following sections (Section 3.2.3).

3.1.4. Injectability and spreadability assessment

The ease of application of systems intended for rectal administration is a key factor influencing the patient acceptability [26]. In this study, we investigated this aspect by evaluating both the injectability and the spreadability index of the formulations.

The formulation prepared with the highest concentration of 5-ASA (0.25% *w*/w) was loaded as a liquid form into a needleless syringe equipped with a Luer slip tip (inner diameter: 4 mm), mimicking the cannula of a microenema, and injected into PBS preheated to 37 °C. As shown in Fig. S6 and Video S3, the formulation was easily extruded and rapidly transitioned into a gel upon contact with the warm medium. While the injectability of P407 systems had already been demonstrated through rheological analysis and their shear-thinning behavior (Section 3.1.1), this practical test together with gelation time measurements further confirmed that the formulation can be easily administered as a liquid form at room temperature, gelling after *in situ* administration [42].

Moreover, the mean spreadibility index of the same formulation was 20 ± 1 mm, confirming that it is easily spreadable under minimal shear, offering a more comfortable application experience (Fig. S6 and Video

S4) [26,42].

3.1.5. FT-IR analysis and evaluation of antioxidant activity

FT-IR spectroscopy confirmed the presence of characteristic functional groups of POE and POP in the samples containing P407 (Fig. 4A and B) [27]. On the contrary, the characteristic absorption bands of 5-ASA, *i.e.* 2500 cm^{-1} (intramolecular hydrogen bonding with a carboxyl group), 1643 cm^{-1} (N—H primary deformation), 1483–1447 cm^{-1} (C═C stretches in the aromatic ring), 1349 cm^{-1} (C—N stretching), 808–685 cm^{-1} (aromatic C—H out of plane bending vibrations), were found to merge with the absorption bands of the copolymeric matrix after its incorporation in the P407 hydrogel, suggesting a conceivable interaction between the drug and the copolymer (Fig. 4A and B) [81–83]. The hydrophobic nature of 5-ASA likely facilitated its partitioning into the hydrophobic regions of the P407 polymer chains. The reorganization of P407 into micelles when the temperature increased probably promoted the solubilization of the active compound within the colloidal structure [31]. These results support the hypothesis that 5-ASA was not only dispersed in the hydrogel but it also interacted with the copolymeric matrix. [17] Similar results were reported by Yan et al., who developed a P407-based hydrogel containing *Ramulus mori* (Sangzhi) alkaloids, derived from mulberry twigs, and observed comparable drug–polymer interactions. [17] Likewise, our research team has previously obtained consistent findings with P407 hydrogels containing rutin, a flavonoid with limited aqueous solubility [27].

5-ASA has been reported to possess effective oxygen free radical scavenging properties, giving it strong antioxidant potential [11]. To assess this activity, the antioxidant capacity of the 5-ASA-loaded P407 hydrogel was evaluated using the DPPH assay, which measures the reduction of the DPPH radical [27]. As shown in Fig. 4C, the incorporation of 5-ASA into the P407-based hydrogel did not significantly affect its radical-scavenging activity (RSA), showing only a slight reduction

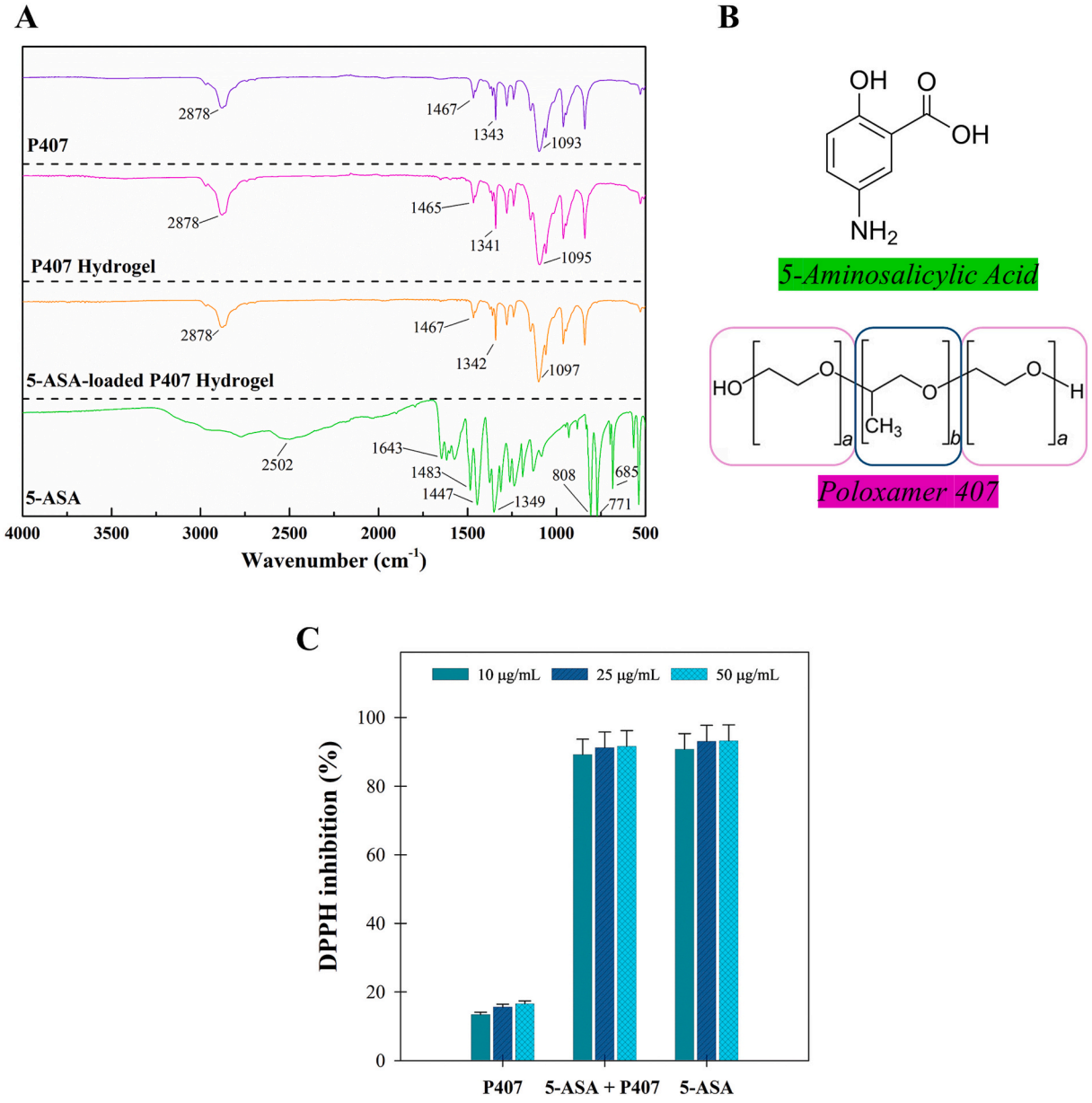

Fig. 4. (A) FT-IR spectra of pure P407, 5-ASA, empty P407 hydrogel (20% w/w), and 5-ASA-loaded P407 hydrogel. (B) Chemical structures of 5-ASA and P407 (a = 101 ethylene oxide units; b = 56 propylene oxide units). (C) Antioxidant activity of the various formulations assessed by the DPPH assay. Results are the average of three independent experiments ± standard deviation. (5-ASA: ethanolic solution; P407: 20% (*w*/w) P407 hydrogel; P407 + 5-ASA: 5-ASA-loaded 20% (w/w) P407 hydrogel).

(~89–91%) compared to the free drug (~91–93%), with RSA values increasing proportionally with the drug concentration. This slight decrease may be attributed to interactions between the antioxidant compound and the polymeric matrix [27]. Notably, the empty P407-based system also exhibited moderate RSA (~13–16%), confirming the data previously reported [84].

The antioxidant properties of 5-ASA are important for the local treatment of IBD, as oxidative stress plays a key role in the pathogenesis and progression of intestinal inflammation [85]. Excessive production of reactive oxygen species (ROS) contributes to mucosal damage, disruption of the epithelial barrier and the amplification of inflammatory responses. 5-ASA can help to decrease the oxidative damage by its scavenging activity, promoting the mucosal healing and enhancing its overall anti-inflammatory effect [85].

3.2. Characterization of P407-5-ASA anti-inflammatory effect in cellular and murine model of IBDs

3.2.1. Anti-inflammatory properties of P407-5-ASA in LPS activated M1 phenotype macrophages

Reliable *in vitro* assessment of anti-inflammatory formulations for treating IBDs requires incorporation of multiple cellular components to reflect the complex, multifactorial nature of intestinal inflammation [86]. To this end, we tested the developed anti-inflammatory formulations in a co-culture system comprising activated macrophages RAW264.7 and Caco-2 cells as a model of immune activation during epithelial inflammation. First, RAW264.7 monocytes were polarized to the M1 pro-inflammatory phenotype by treatment with the bacterial antigen lipopolysaccharide (LPS, 200 ng/mL for 24 h). As expected, the macrophages developed a foam-like morphology (Fig. 5A) and displayed increased expression levels of the M1 marker such as inducible nitric oxide synthase (iNOS) and p-ERK [54] (Fig. 5B). LPS-activated macrophages were then co-cultured with Caco-2 cells in Boyden chamber and their ability to invade Matrigel, as model the extracellular matrix, was

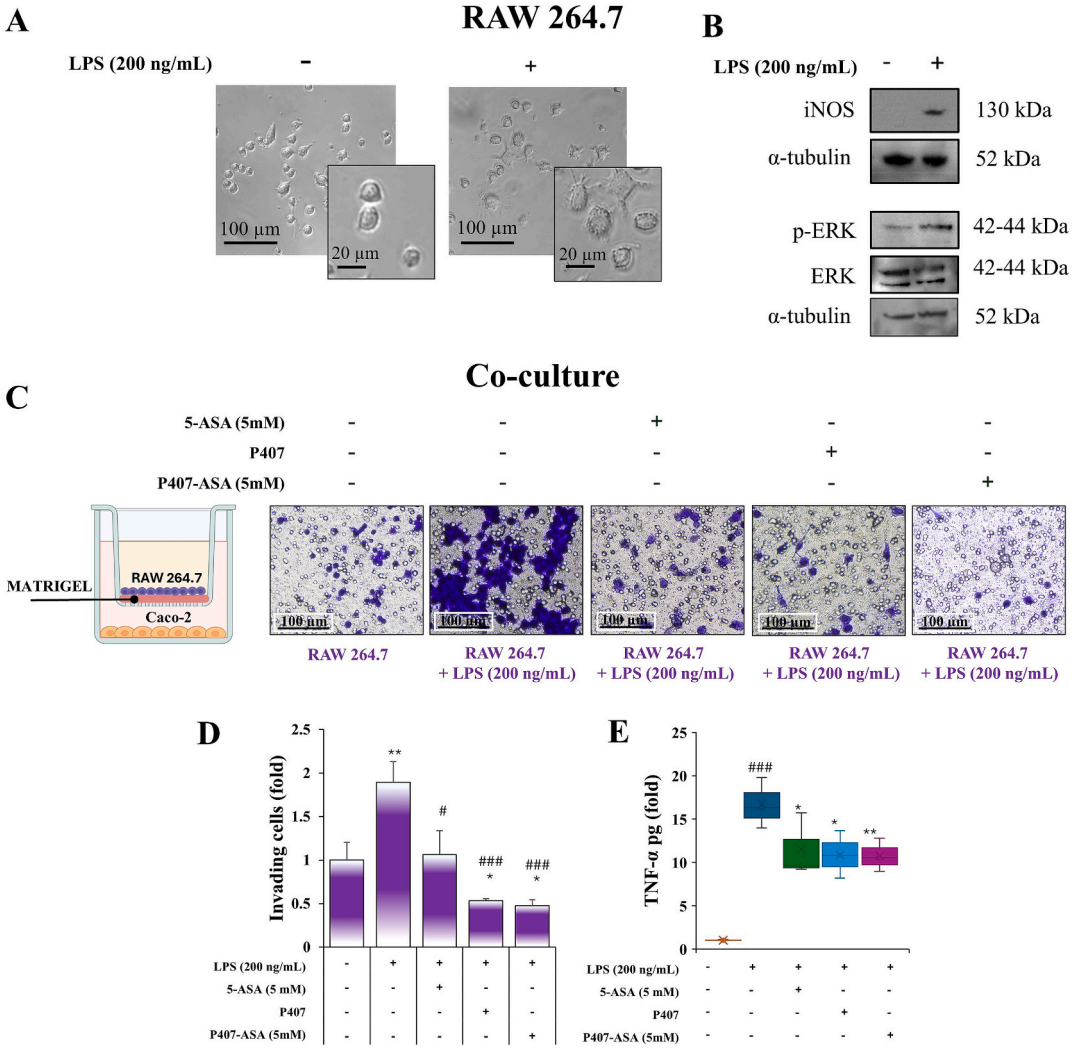

Fig. 5. P407 and mesalazine-loaded P407 hydrogel (P407-5-ASA) treatment of Caco-2 cells strongly decreased invasiveness and ameliorated the inflammation of activated RAW 264.7 macrophages in co-culture. LPS induced the polarization of RAW 264.7 macrophages at M1 phenotype determining (A) altered cellular morphology and (B) increased expression levels of iNOS and p-ERK, as from western blotting; α-tubulin was used as loading control. (C) Invasion assay of RAW 264.7 towards Caco-2 cells in Boyden chambers (pore size 8 µm), pre-coated with matrigel, for 48 h. Representative images are showed. Images were acquired with an inverted light microscope at 10× magnification. (D) After invasion, invading cells were counted, and their number was reported as fold of invading non-activated macrophages. (E) After co-culture TNF-α levels in RAW 264.7 culture medium was quantified by ELISA (Mouse TNF-alpha ELISA PRO) and reported as fold of TNF-α released by non- activated macrophages. (* Statistics with respect to non-activated RAW 264.7 * $p < 0.05$, ** $p < 0.005$, *** $p < 0.0005$; # Statistics with respect to activated RAW 264.7 # $p < 0.05$, # $p < 0.005$, ### $p < 0.0005$).

evaluated. As shown in Fig. 5C, the activated macrophages displayed significantly higher invasion potential than the M0 macrophages. Interestingly, the treatment of Caco-2 cells with the anti-inflammatory formulation P407-5-ASA significantly reduced this effect to a greater extent than the free drug at the same concentration (Fig. 5D). It is worth noting that the P407 hydrogel formulation could also reduce macrophage infiltration to a certain extent, possibly thanks to the well-known anti-inflammatory properties of poloxamer.

Furthermore, co-culturing LPS-activated macrophages with Caco-2 cells resulted in a significant increase in the release of the pro-inflammatory cytokine TNF-α in the basolateral compartment of the Boyden chamber, as expected from inflammation induction by activated macrophages (Fig. 5E). TNF-α levels were significantly reduced in the presence of anti-inflammatory treatment. Notably, this reduction was more pronounced in P407 and P407-5-ASA-treated cells than in cells treated with the free drug at the same concentration, thus proving the greater anti-inflammatory potential of the developed P407-based formulations compared to the free form of active compound.

Moreover, the cytocompatibility of both P407 and P407-5-ASA was confirmed in human fibroblasts, used as a representative non-transformed cell line, as evaluated by MTT assay (Fig. S8).

3.2.2. *Anti-inflammatory properties of P407-5-ASA in an optimized in vitro model of inflamed colon epithelium*

Increasing attention has been committed to experimental models of intestinal microenvironment, including immune-epithelial interactions and dynamic inflammatory signaling, which are essential to predict the therapeutic efficacy of the experimental formulations in complex diseases such as IBD [87].

In this contest, Caco-2 cells, thanks to their stability in culture and ability to spontaneously polarize into intestinal enterocytes (iECs), are a convenient and widely available model of the intestinal epithelium [49]. In this study, we established a prolonged culture of Caco-2 cells (14–21 days) that enabled intestinal enterocyte differentiation, providing an optimized platform for testing anti-inflammatory treatments. *Z*-stack acquisitions and 3D volume reconstruction confirmed the development of domes and microvilli, which are hallmarks of differentiated iECs (Fig. S9A and B) [86].

In an initial investigation of the anti-inflammatory potential of P407-based formulations on differentiated Caco-2 cells, the monolayers were exposed to LPS as an inflammation-triggering agent. Prolonged exposure of the monolayers to LPS (72 h) caused their complete disruption (Fig. S10). 5-ASA was unable to prevent this effect, whereas both P407

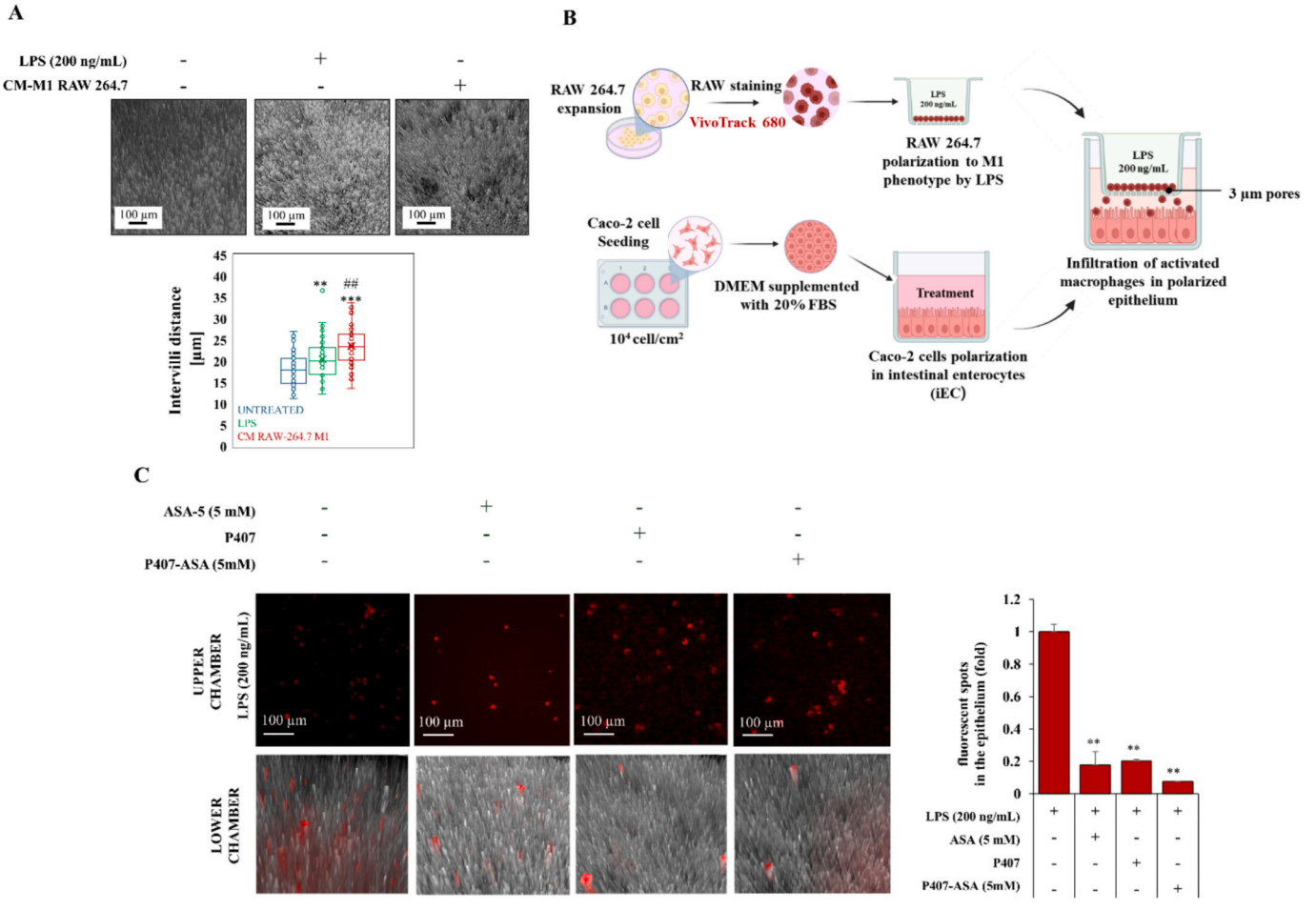

Fig. 6. P407 and P407-5-ASA treatment significantly reduced macrophage infiltration in an *in vitro* model of inflamed small-intestine by co-culture of differentiated Caco-2 in iECs and LPS-activated RAW 264.7 macrophages. Caco-2 cells were differentiated in iECs by prolonged culture (14–21 days) and (A) z-stack images confirmed villi development after 21 days of culture. Inter-villi distance in untreated differentiated Caco-2 monolayer was evaluated by ImageJ software and compared with the same distance measured in presence of LPS (200 ng/mL, 24 h) or the conditioned medium (CM) from LPS-activated RAW 264.7 macrophages to confirm inflammation. The model was established in Boyden chamber (pore size 3 µm) as sketched in (A). Activated RAW 264.7 were stained with Vivotrack 680 to follow their infiltration in iECs treated or not with free 5-ASA, P407 gel or P407-5-ASA (5mM drug) over time. (B) Live images of infiltrating cells after 24 hour of co-culture were acquired with an inverted fluorescent microscope (Ti2 Eclipse, Nikon) at 10× magnification and representative images are reported. (C) Number of infiltrating macrophages was quantified by ImageJ software and reported as fold of infiltrating RAW 264.7 in untreated differentiated iECs. * Statistics with respect to untreated differentiated Caco-2 monolayer ** $p < 0.005$, *** $p < 0.0005$; # Statistics with respect to LPS-treated differentiated Caco-2 monolayer ## $p < 0.005$.

and P407-5-ASA preserved monolayer integrity (Fig. S10). Next, we tested the anti-inflammatory potential of P407-5-ASA in an optimized co-culture of LPS-activated macrophages and differentiated Caco-2 cells in iECs. When iECs were exposed to LPS or conditioned medium (CM) from LPS-activated RAW 264.7 cells for 24 hour morphological alterations of the monolayers were observed. In particular, inflammation induced villi damage as demonstrated by a significant increase of the inter-villi distance (Fig. 6A). Notably, this effect was strongly exacerbated by CM from LPS-activated RAW 264.7 cells, as evidenced by the markedly increased inter-villi distance compared to LPS-treated monolayers and the formation of distinct regions of disrupted barrier. Thus, we demonstrated the ability of LPS-activated macrophages to propagate inflammation to differentiated epithelium and we established the co-culture of LPS-activated RAW 264.7 and differentiated Caco-2 in iECs (Fig. 6B) as an optimized model of intestinal inflammation. RAW 264.7 macrophages were labeled with Vivotrack-680 for tracking their migration across the trans-well insert and infiltration into differentiated colon epithelium cellular model over time. As shown in Fig. 6C, anti-inflammatory treatment with P407-5-ASA caused the most drastic reduction in the number of infiltrating macrophages compared to P407 and 5-ASA used as single components, as demonstrated by the increase in the number of macrophages in the upper chamber and the reduction in the number of fluorescent spots in the differentiated iECs. These results confirmed the superior anti-inflammatory properties of P407-5-ASA *in vitro* with respect to the free form of the active compound, that can be attributed to the sustained drug release, as well as to the mild inflammatory nature of the poloxamer [27,88,89].

3.2.3. *Therapeutic efficacy of P407-5-ASA in IBD murine model*

To evaluate the colon-adhesive *in vivo* property of P407-based formulation, high frequency ultrasound-guided (HFSU) rectal administration of rhodamine-loaded gel was performed in CD1 mice. This allowed us to precisely evaluate hydrogel deposition and its colon-retention over time [90]. HFSU image showed the localization of the gel into the colon-rectum upon administration where it appeared as a hyperechoic region (red arrow in Fig. S11A) and this was confirmed by

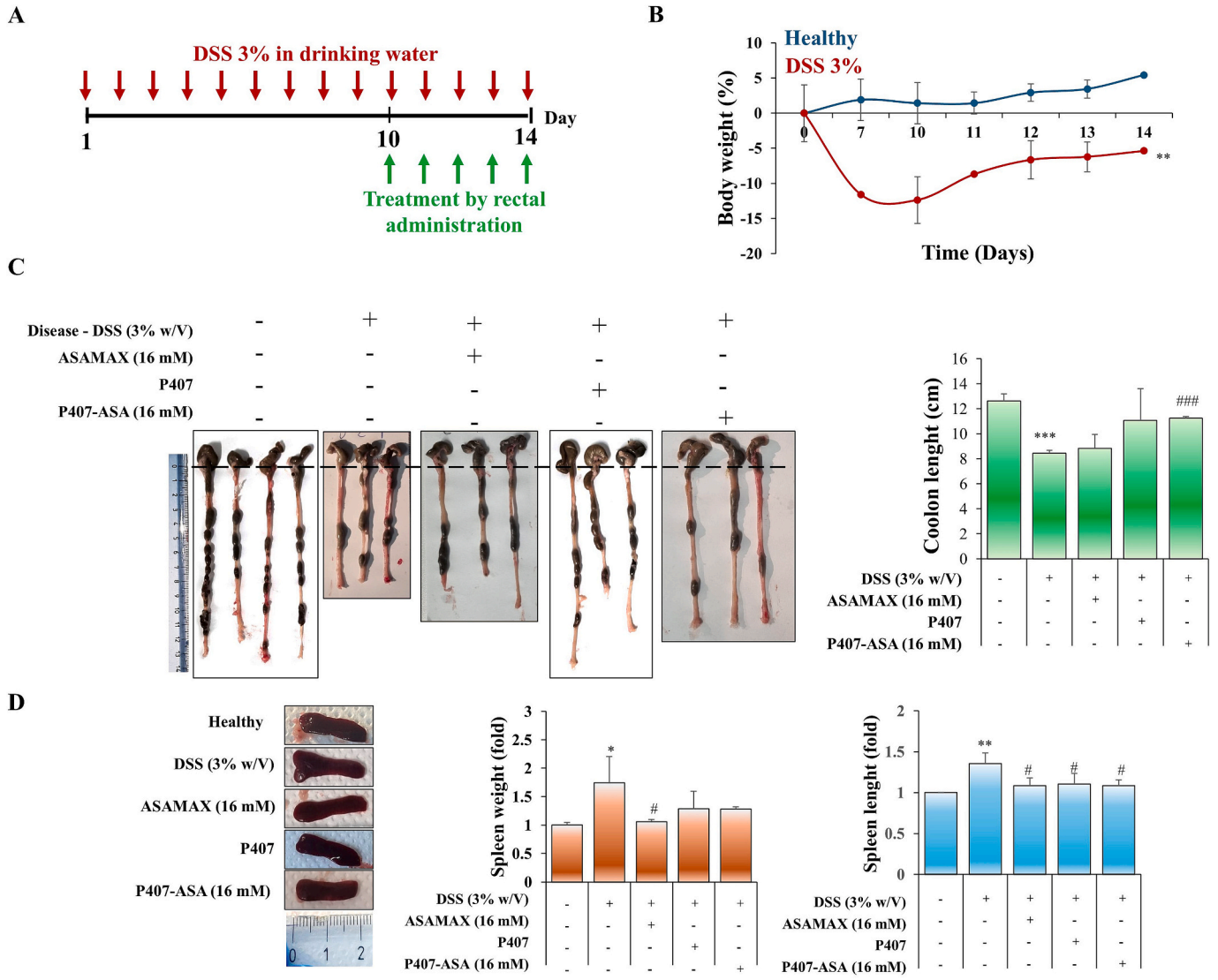

Fig. 7. P407-5-ASA reduced the inflammation in a murine model of IBD. A) Treatment schedule for the establishment of DSS-induced UC in CD1 mice as well as for the anti-inflammatory treatment; B) DSS-induced reduction of mice body weight over the treatment time frame; C) Representative images of length of excised colons ($n = 3$ for each treatment) from euthanized mice at the end of treatment; D) Quantification of the effect of DSS and the different treatments on colon length; D) Representative images of spleen from different treatment groups at the end of the treatment and their relative weight and length. * Statistics with respect to healthy untreated mice, ** $p < 0.005$, *** $p < 0.0005$; # Statistics with respect to UC-bearing mice # $p < 0.05$, ### $p < 0.0005$. DSS 3%: mice treated with 3% low molecular weight dextran sodium sulfate salt in drinking water (Section 2.3.7).

fluorescent *in vivo* imaging (Fig. S11B). After 3 h administration, mice were euthanized and the hydrogel was still identified in the final tract of the colon by *ex vivo* fluorescent imaging, despite a reduced fluorescent signal being detected (Fig. S12A). This confirmed the ability of the hydrogel to be retained over time and the progressive release of its cargo (*i.e.* rhodamine). *Ex vivo* images of colon 24 h after administration showed that the gel was completely cleared (Fig. S12B).

The *in vivo* therapeutic potential of the anti-inflammatory P407-based formulations was evaluated in a DSS-induced ulcerative colitis murine model. Low molecular weight DSS is a widely recognized chemical inducer of ulcerative colitis in pre-clinical animal model [13,54]. UC was induced in CD1 mice by dissolving DSS 3% *w/v* in drinking water that was administered according to the schedule in Fig. 7A. To follow disease establishment and progression, animals were weighed to check for weight loss and monitored for stool consistency as well as onset of rectal bleeding, daily. The evaluation of these parameters allowed the estimation of the Disease Activity Index (DAI) which was scored as reported in Table S3. After 7 days of treatment, DSS-treated mice lost about 12% of their body weight whereas untreated animals gained weight, as expected from normal growth (Fig. 7B). On day 10 DAI reached the highest score (Table S4) and for this reason was selected as the starting point for anti-inflammatory treatment administration. UC-bearing mice were randomized in four groups as follows: untreated ($n = 3$), and treated with ASAMAX (n = 3), P407 (n = 3), P407-5-ASA (n = 3). Treatments were administered rectally, daily, and for five days by the injection of 50 μL of ASAMAX in Vaseline oil or P407 or P407-5-ASA. DSS 3% w/v caused a significant reduction in colon length compared to the control (Fig. 7C), as well as poor stool retention, thus confirming disease establishment [91]. Treatment of mice with P407-5-ASA caused a significant recovery of colon length, higher than ASAMAX alone at the same concentration (16 mM) as shown in Fig. 7C. The treatment of mice with P407 alone caused a partial but not significant recovery of colon length (Fig. 7C). Moreover, spleen from different groups were collected, weighted and their length measured being spleen enlargement a sign of systemic inflammation commonly observed following DSS treatment [54,92]. Results in Fig. 7D showed, as expected, a significant increase in spleen length and weight in DSS treated mice with respect to healthy control. This effect was restored by all the anti-inflammatory treatments. Overall, these findings demonstrate that the superiority of the thermosensitive formulation is more evident at the local colon compartment rather than at the systemic level, probably as a consequence of the prolonged tissue residence time and sustained drug release.

Moreover, at the end of the treatment, P407-5-ASA and ASAMAX strongly reduced the DAI that was only ameliorated by P407 (Table S4). These results confirmed the *in vitro* observations regarding the significant therapeutic efficacy of P407-5-ASA, attributable to its greater accumulation and retention in the inflamed colon tissue thanks to its mucoadhesive properties and gradual release of the drug over time.

Despite these promising therapeutic outcomes, further investigations are required to assess the local safety profile of the proposed formulation after multiple rectal administrations. P407 is a well-known and biocompatible excipient, and several previous experimental studies have shown its safety when employed as component of thermosensitive rectal or mucosal delivery systems; for example, histological evaluations demonstrated the absence of significant mucosal damage or irritation, as well as the preservation of rectal tissue integrity following intrarectal administration in animal models, thereby supporting its suitability for local drug delivery applications [43,72,93,94].

Liu and *co*-workers developed a thermosensitive *in situ* gel based on poloxamer combined with mucoadhesive polymers for the rectal delivery of ibuprofen, demonstrating improved pharmacokinetic profiles together with the absence of significant mucosal irritation, as confirmed by histopathological analyses following rectal administration in rabbits, thereby supporting the feasibility and local safety of poloxamer-based rectal gels [43]. Similarly, studies on poloxamer gels containing diclofenac sodium have demonstrated that their rectal administration can promote a faster drug absorption, maintaining a safety profile comparable to that of conventional semi-solid suppositories, with no morphological alterations observed in rectal tissues of treated animals [93].

Nevertheless, considering the inflamed and ulcerated conditions characteristic of IBD, future studies including histopathological analyses of colorectal tissues will be essential to further corroborate the local tolerability of the proposed formulations and to strengthen the translational relevance of the P407-5-ASA system.

4. Conclusion

This study demonstrated the potential of P407-based hydrogels as useful formulations for the rectal administration for 5-ASA for the treatment of IBD.

The liquid suppository developed in this study met the key requirements for an ideal rectal formulation, including appropriate gelation temperature and time, muco-adhesive properties, adequate gel strength, good injectability and spreadability. Additionally, the formulation did not compromise the antioxidant activity of 5-ASA, which is considered crucial for IBD therapy. *In vitro* release studies showed prolonged drug retention and sustained release of 5-ASA even under acidic pH conditions, which may occur during active phases of IBD.

In preclinical models of IBD, both in the optimized co-culture cell model and in DSS-induced acute colitis in mice, P407-5-ASA showed improved and superior therapeutic efficacy compared to the free form of the drug. It was demonstrated by its ability to reduce M1 macrophage infiltration into the inflamed epithelium and TNF-α release. These results were validated by *in vivo* studies that demonstrated greater accumulation, retention and therapeutic effect of P407-5-ASA in inflamed colon tissue due to its mucoadhesive properties and gradual release of the drug over time.

Overall, these results suggest that the P407 hydrogel containing 5-ASA is a promising formulation to be employed for the management of IBD.

However, additional preclinical studies are needed to confirm the safety, efficacy and targeted release of the drug before moving onto the clinical phase. In fact, despite the obtained promising results, some limitations and criticisms need to be addressed. First of all, the proposed system relies on a simple single-polymer P407-based hydrogel in comparison with more complex delivery systems used for the rectal administration of 5-ASA, such as multi-component formulations [95–98], While this simplicity represents a clear advantage in terms of formulation reproducibility, solvent-free preparation, scalability and translational potential, as well as the absence of specialized or complex manufacturing equipment, it also highlights the need of additional investigations of specific aspects relevant to clinical application.

From a biological standpoint, the *in vitro* inflammatory model was designed to provide a robust and reproducible macrophage-mediated inflammatory stimulus for downstream epithelial studies. Accordingly, TNF-α was selected as a representative and well-established pro-inflammatory cytokine. Nevertheless, a more comprehensive characterization of macrophage polarization, including the assessment of additional pro-inflammatory cytokines (*e.g.*, IL-6 and IL-1β), phenotypic markers of M1/M2 activation (such as CD80 and CD206) and intracellular oxidative stress (ROS levels) would further strengthen the mechanistic understanding of the anti-inflammatory effects observed.

In addition, although P407 is generally recognized as safe and widely used for topical, mucosal and injectable formulations, the local tolerability of multiple rectal administrations of the formulation at relatively high polymer concentrations, especially in the presence of inflamed or ulcerated colonic mucosa, needs to be evaluated. Future preclinical studies should therefore include systematic safety assessments, such as histopathological analysis of colorectal tissue following repeated administrations, in order to demonstrate the absence of local irritation or

mucosal damage and to fully support the translational potential of this P407-based hydrogel system. Last but not least, the present *in vivo* investigation was carried out as an initial proof-of-concept using a limited number of animals per group, in accordance with the 3Rs principles. Even though the observed therapeutic trends were consistent, future studies involving larger animal cohorts will be necessary to strengthen statistical power and further validate the efficacy and safety of the proposed formulation.

CRediT authorship contribution statement

Elena Giuliano: Writing – review & editing, Writing – original draft, Software, Methodology, Investigation, Formal analysis, Data curation, Conceptualization. **Angela Costagliola di Polidoro:** Writing – review & editing, Writing – original draft, Software, Project administration, Investigation, Formal analysis, Conceptualization. **Agnese Gagliardi:** Writing – review & editing, Visualization, Methodology, Formal analysis. **Domenico Sorrentino:** Writing – review & editing, Methodology, Investigation, Formal analysis. **Emanuela Longo:** Writing – review & editing, Software, Formal analysis, Data curation. **Sandra Albanese:** Writing – review & editing, Visualization, Validation, Formal analysis. **Francesco Napolitano:** Writing – review & editing, Visualization, Validation, Methodology. **Valeria Gaetano:** Writing – review & editing, Supervision, Software, Investigation. **Antonella Zannetti:** Writing – review & editing, Validation, Supervision, Resources, Methodology, Funding acquisition, Conceptualization. **Donato Cosco:** Writing – review & editing, Visualization, Validation, Resources, Project administration, Funding acquisition, Data curation, Conceptualization.

Declaration of competing interest

The authors declare that they have no known competing financial interests or personal relationships that could have appeared to influence the work reported in this paper.

Acknowledgments

This work was supported by the Italian Ministry of University and Research (PRIN2022_PNRR, protocol no. P202242HYK).

Appendix A. Supplementary data

Supplementary data to this article can be found online at https://doi.org/10.1016/j.bioadv.2026.214762.

Data availability

Data will be made available on request.

References

[1] A. Aljabri, G.M. Soliman, Y.N. Ramadan, M.A. Medhat, H.F. Hetta, Biosimilars versus biological therapy in inflammatory bowel disease: challenges and targeting strategies using drug delivery systems, Clin. Exp. Med. 25 (2025) 107, https://doi.org/10.1007/s10238-025-01558-6.
[2] A. Gagliardi, M. Del Valle, S. Espuelas, J.M. Irache, D. Cosco, Application of zein nanoparticles for the treatment of inflammatory bowel diseases, Expert Opin. Drug Deliv. (2025) 1–16, https://doi.org/10.1080/17425247.2025.2527693.
[3] P.M. Veloso, R. Machado, C. Nobre, Mesalazine and inflammatory bowel disease – from well-established therapies to progress beyond the state of the art, Eur. J. Pharm. Biopharm. 167 (2021) 89–103, https://doi.org/10.1016/j.ejpb.2021.07.014.
[4] W. Sun, Z. Li, X. Zhang, Q. Luo, L. Wei, C. Xiao, Biomaterial-based therapeutic strategies for inflammatory bowel disease, Biomaterials 324 (2026) 123462, https://doi.org/10.1016/j.biomaterials.2025.123462.
[5] V.K. Shahgoli, S. Noorolyai, M. Ahmadpour Youshanlui, H. Saeidi, H. Nasiri, B. Mansoori, U. Holmskov, B. Baradaran, Inflammatory bowel disease, colitis, and cancer: unmasking the chronic inflammation link, Int. J. Color. Dis. 39 (2024) 173, https://doi.org/10.1007/s00384-024-04748-y.
[6] E.M. Jacob, A. Borah, S.C. Pillai, D.S. Kumar, Inflammatory bowel disease: the emergence of new trends in lifestyle and nanomedicine as the modern tool for pharmacotherapy, Nanomaterials 10 (2020), https://doi.org/10.3390/nano10122460.
[7] Y. Ouyang, J. Zhao, S. Wang, Multifunctional hydrogels based on chitosan, hyaluronic acid and other biological macromolecules for the treatment of inflammatory bowel disease: a review, Int. J. Biol. Macromol. 227 (2023) 505–523, https://doi.org/10.1016/j.ijbiomac.2022.12.032.
[8] S. Voci, A. Gagliardi, N. Ambrosio, A. Zannetti, D. Cosco, Lipid- and polymer-based formulations containing TNF-α inhibitors for the treatment of inflammatory bowel diseases, Drug Discov. Today 29 (2024) 104090, https://doi.org/10.1016/j.drudis.2024.104090.
[9] Q. Pan, L. Xie, P. Cai, D. Wu, H. Zhu, L. Xu, R. Liu, K. Luo, B. He, Y. Pu, Acid-resistant nano-antioxidants based on epigallocatechin gallate alleviate acute intestinal and kidney inflammation, ACS Appl. Mater. Interfaces 16 (2024) 46090–46101, https://doi.org/10.1021/acsami.4c09901.
[10] I. Ahmed Najar, A. Sharma, A. Alshammari, T.H. Albekairi, M. Alharbi, T. Ahmad Dar, Z. Latief Qadrie, A. Kabra, A.M.J. Newton, M. Kumar, Anti-oxidant and anti-inflammatory potential of different polymer-based mesalamine delayed-release granules in TNBS-induced ulcerative colitis in wistar rats, Saudi Pharm. J. 32 (2024) 101910, https://doi.org/10.1016/j.jsps.2023.101910.
[11] Y. Wu, S. Li, M. Jin, D. Li, Z. Zhou, H. Hou, Y. Han, Preparation of MSZ hydrogel and its treatment of colitis, Front. Pharmacol. 12 (2021), https://doi.org/10.3389/fphar.2021.706401.
[12] T. Xiao, Z. Yu, H. Yang, J. You, X. Wu, Marine polysaccharides hydrogel with encapsulated mesalazine for the treatment of ulcerative colitis: integrative effects on inflammation, microbiota, and mucosal repair, Colloids Surf. B: Biointerfaces 253 (2025) 114722, https://doi.org/10.1016/j.colsurfb.2025.114722.
[13] E. Palma, N. Costa, R. Molinaro, M. Francardi, D. Paolino, D. Cosco, M. Fresta, Improvement of the therapeutic treatment of inflammatory bowel diseases following rectal administration of mesalazine-loaded chitosan microparticles vs Asamax(®), Carbohydr. Polym. 212 (2019) 430–438, https://doi.org/10.1016/j.carbpol.2019.02.049.
[14] J. Zhang, C. Wang, X. Wu, Y. Lin, Alleviating ulcerative colitis via rectal administration: enhancing the therapeutic effects of silk sericin-proanthocyanidins nanoparticles with a Poloxamer thermosensitive in situ gel, Int. J. Pharm.: X 9 (2025) 100337, https://doi.org/10.1016/j.ijpx.2025.100337.
[15] C. Lei, J. Wen, Y. Sun, M. Ren, R. Qiao, C. Li, Self-assembled herbal hydrogel for rectal administration therapy in ulcerative colitis, Chem. Eng. J. 503 (2025) 158477, https://doi.org/10.1016/j.cej.2024.158477.
[16] S. Hu, R. Zhao, Y. Xu, Z. Gu, B. Zhu, J. Hu, Orally-administered nanomedicine systems targeting colon inflammation for the treatment of inflammatory bowel disease: latest advances, J. Mater. Chem. B 12 (2024) 13–38, https://doi.org/10.1039/D3TB02302H.
[17] Y. Yan, J. Song, D. Liu, Z. Liu, J. Cheng, Z. Chen, Y. Yang, W. Jiang, H. Wang, J. Ye, Y. Liu, Simple and versatile in situ thermo-sensitive hydrogel for rectal administration of SZ-A to alleviate inflammation and repair mucosal barrier in ulcerative colitis, Chin. Chem. Lett. 35 (2024) 109736, https://doi.org/10.1016/j.cclet.2024.109736.
[18] E. Giuliano, D. Paolino, M. Fresta, D. Cosco, Mucosal applications of poloxamer 407-based hydrogels: an overview, Pharmaceutics (2018), https://doi.org/10.1039/D3TB02302H.10.3390/pharmaceutics10030159.
[19] B. Khan, A. Arbab, S. Khan, H. Fatima, I. Bibi, N.P. Chowdhry, A.Q. Ansari, A. A. Ursani, S. Kumar, J. Hussain, S. Abdullah, Recent progress in thermosensitive hydrogels and their applications in drug delivery area, MedComm – Biomaterials and Applications 2 (2023) e55, https://doi.org/10.1002/mba2.55.
[20] Hydrogel-exosome systems in the treatment of refractory diabetic ulcers: mechanisms, progress, and prospects, Eur. Cell. Mater. 53 (2025) 82–97, https://doi.org/10.22203/eCM.v053a07.
[21] Y. Guo, W. Min, Z. Yuzhong, Z. Zeyun, J. Li, Advanced hydrogel material for colorectal cancer treatment, Drug Deliv. 32 (2025) 2446552, https://doi.org/10.1080/10717544.2024.2446552.
[22] G. Dumortier, J.L. Grossiord, F. Agnely, J.C. Chaumeil, A review of poloxamer 407 pharmaceutical and pharmacological characteristics, Pharm. Res. 23 (2006) 2709–2728, https://doi.org/10.1007/s11095-006-9104-4.
[23] R. Jaquilin P J, O.S. Oluwafemi, S. Thomas, A.O. Oyedeji, Recent advances in drug delivery nanocarriers incorporated in temperature-sensitive Pluronic F-127–a critical review, J. Drug Deliv. Sci. Technol. 72 (2022) 103390, https://doi.org/10.1016/j.jddst.2022.103390.
[24] E. Giuliano, D. Paolino, M.C. Cristiano, M. Fresta, D. Cosco, Rutin-loaded poloxamer 407-based hydrogels for in situ administration: stability profiles and rheological properties, Nanomaterials 10 (2020) 1069, https://doi.org/10.3390/nano10061069.
[25] E. Ban, M. Park, S. Jeong, T. Kwon, E.H. Kim, K. Jung, A. Kim, Poloxamer-based thermoreversible gel for topical delivery of emodin: influence of P407 and P188 on solubility of emodin and its application in cellular activity screening, Molecules 22 (2017) 246, https://doi.org/10.3390/molecules22020246.
[26] L. Djekic, B. Čalija, Đ. Medarević, Gelation behavior, drug solubilization capacity and release kinetics of poloxamer 407 aqueous solutions: the combined effect of copolymer, cosolvent and hydrophobic drug, J. Mol. Liq. 303 (2020) 112639, https://doi.org/10.1016/j.molliq.2020.112639.
[27] E. Giuliano, A. Gagliardi, A. Farhan, S. Voci, N. Costa, S. Bulotta, V. Mollace, E. Palma, M. Majid, D. Cosco, Poloxamer 407-based hydrogels containing rutin increase the in vitro and in vivo wound healing phenomena, ACS Appl. Bio Mater. 8 (2025) 1972–1983, https://doi.org/10.1021/acsabm.4c01452.

[28] E. Giuliano, M. Fresta, D. Cosco, Development and characterization of poloxamine 908-hydrogels for potential pharmaceutical applications, J. Mol. Liq. 337 (2021) 116588, https://doi.org/10.1016/j.molliq.2021.116588.
[29] L. Zou, Y. Hou, X. Nie, S. Wang, S. Tian, Z. Sun, Z. Sun, X. Xu, G. Li, G. Ma, H. Liu, All-small-molecule supramolecular hydrogel combining self-delivery and ROS-responsive release for inhibiting tumor growth and postoperative recurrence, ACS Appl. Mater. Interfaces 17 (2025) 13494–13512, https://doi.org/10.1021/acsami.4c20852.
[30] E. Giuliano, E. Longo, A. Gagliardi, S. Costa, F. Squillace, S. Voci, M. Verdiglione, D. Cosco, Development and characterization of niaprazine-loaded xanthan gum-based gel for oral administration, Gels 11 (2025), https://doi.org/10.3390/gels11020101.
[31] R.S.C.M.Q. Antonino, T.L. Nascimento, E.R. de Oliveira Junior, L.G. Souza, A. C. Batista, E.M. Lima, Thermoreversible mucoadhesive polymer-drug dispersion for sustained local delivery of budesonide to treat inflammatory disorders of the GI tract, J. Control. Release 303 (2019) 12–23, https://doi.org/10.1016/j.jconrel.2019.04.011.
[32] A. Račić, B.J. Dukovski, J. Lovrić, V. Dobričić, S. Vučen, A. Micov, R. Stepanović-Petrović, M. Tomić, U. Pecikoza, J. Bajac, Synergism of polysaccharide polymers in antihistamine eye drops: influence on physicochemical properties and in vivo efficacy, Int. J. Pharm. 655 (2024) 124033, https://doi.org/10.1016/j.ijpharm.2024.124033.
[33] C. Pagano, S. Giovagnoli, L. Perioli, M.C. Tiralti, M. Ricci, Development and characterization of mucoadhesive-thermoresponsive gels for the treatment of oral mucosa diseases, Eur. J. Pharm. Sci. 142 (2020) 105125, https://doi.org/10.1016/j.ejps.2019.105125.
[34] L. Mayol, F. Quaglia, A. Borzacchiello, L. Ambrosio, M.I. La Rotonda, A novel poloxamers/hyaluronic acid in situ forming hydrogel for drug delivery: rheological, mucoadhesive and in vitro release properties, Eur. J. Pharm. Biopharm. 70 (2008) 199–206, https://doi.org/10.1016/j.ejpb.2008.04.025.
[35] J. Ceulemans, I. Vinckier, A. Ludwig, The use of xanthan gum in an ophthalmic liquid dosage form: rheological characterization of the interaction with mucin, J. Pharm. Sci. 91 (2002) 1117–1127, https://doi.org/10.1002/jps.10106.
[36] L. Zhang, D.L. Parsons, C. Navarre, U.B. Kompella, Development and in-vitro evaluation of sustained release Poloxamer 407 (P407) gel formulations of ceftiofur, J. Control. Release 85 (2002) 73–81, https://doi.org/10.1016/S0168-3659(02)00273-0.
[37] W. Wang, P.C.L. Hui, E. Wat, F.S.F. Ng, C.W. Kan, X. Wang, E.C.W. Wong, H. Hu, B. Chan, C.B.S. Lau, P.C. Leung, In vitro drug release and percutaneous behavior of poloxamer-based hydrogel formulation containing traditional Chinese medicine, Colloids Surf. B Biointerfaces 148 (2016) 526–532, https://doi.org/10.1016/j.colsurfb.2016.09.036.
[38] A. Gagliardi, E. Chiarella, S. Voci, N. Ambrosio, M. Celano, M. Cristina Salvatici, D. Cosco, DIFUCOSIN: DIclofenac sodium salt loaded FUCOidan-SericIN nanoparticles for the management of chronic inflammatory diseases, Int. J. Pharm. 655 (2024) 124034, https://doi.org/10.1016/j.ijpharm.2024.124034.
[39] M. Suhail, M.C. Hung, I.H. Chiu, Q.L. Vu, P.C. Wu, Preparation and in-vitro characterization of 5-aminosalicylic acid loaded hydrogels for colon specific delivery, J. Mater. Res. Technol. 21 (2022) 339–352, https://doi.org/10.1016/j.jmrt.2022.09.031.
[40] J. Dai, W. Long, Z. Liang, L. Wen, F. Yang, G. Chen, A novel vehicle for local protein delivery to the inner ear: injectable and biodegradable thermosensitive hydrogel loaded with PLGA nanoparticles, Drug Dev. Ind. Pharm. 44 (2018) 89–98, https://doi.org/10.1080/03639045.2017.1373803.
[41] S. Fattahpour, M. Shamanian, N. Tavakoli, M. Fathi, H. Sadeghi-Aliabadi, S. R. Sheykhi, M. Fesharaki, S. Fattahpour, An injectable carboxymethyl chitosan-methylcellulose-pluronic hydrogel for the encapsulation of meloxicam loaded nanoparticles, Int. J. Biol. Macromol. 151 (2020) 220–229, https://doi.org/10.1016/j.ijbiomac.2020.02.002.
[42] F. Firoz, T. Yousef, Y. Asser, R.M. Thaer, R.M.F. Sammour, Thermo-activated in situ rectal gel preparation for ibuprofen using eutectic mixture, Eur. J. Pharm. Sci. 200 (2024) 106843, https://doi.org/10.1016/j.ejps.2024.106843.
[43] Y. Liu, X. Wang, Y. Liu, X. Di, Thermosensitive in situ gel based on solid dispersion for rectal delivery of ibuprofen, AAPS PharmSciTech 19 (2018) 338–347, https://doi.org/10.1208/s12249-017-0839-5.
[44] A. Gagliardi, E. Giuliano, S. Voci, N. Costa, S. Bulotta, M.C. Salvatici, N. Ambrosio, D. Paolino, F. Siddique, M. Majid, E. Palma, M. Fresta, D. Cosco, Rutin-loaded zein gel as a green biocompatible formulation for wound healing application, Int. J. Biol. Macromol. 269 (2024) 132071, https://doi.org/10.1016/j.ijbiomac.2024.132071.
[45] A. Lupu, M. Bercea, M. Avadanei, L.M. Gradinaru, L.E. Nita, V.R. Gradinaru, Temperature sensitive Pluronic F127-based gels incorporating natural therapeutic agents, Macromol. Mater. Eng. 310 (2025) 2400341, https://doi.org/10.1002/mame.202400341.
[46] A. Zannetti, F. Iommelli, A. Speranza, M. Salvatore, S. Del Vecchio, 3′-deoxy-3′-¹⁸F-fluorothymidine PET/CT to guide therapy with epidermal growth factor receptor antagonists and Bcl-x_L inhibitors in non–small cell lung cancer, J. Nucl. Med. (2012) jnumed.111.096503, https://doi.org/10.2967/jnumed.111.096503.
[47] A. Zannetti, F. Iommelli, R. Fonti, A. Papaccioli, J. Sommella, A. Lettieri, G. Pirozzi, R. Bianco, G. Tortora, M. Salvatore, S. Del Vecchio, Gefitinib induction of in vivo detectable signals by Bcl-2/Bcl-xL modulation of inositol trisphosphate receptor type 3, Clin. Cancer Res. 14 (2008) 5209–5219, https://doi.org/10.1158/1078-0432.CCR-08-0374.
[48] S. Camorani, S. Tortorella, L. Agnello, C. Spanu, A. d'Argenio, R. Nilo, A. Zannetti, E. Locatelli, M. Fedele, M. Comes Franchini, L. Cerchia, Aptamer-functionalized nanoparticles mediate PD-L1 siRNA delivery for effective gene silencing in triple-negative breast cancer cells, Pharmaceutics 14 (2022), https://doi.org/10.3390/pharmaceutics14102225.
[49] S. Schnur, V. Wahl, J.K. Metz, J. Gillmann, F. Hans, K. Rotermund, R.-K. Zäh, D. A. Brück, M. Schneider, M. Hittinger, Inflammatory bowel disease addressed by Caco-2 and monocyte-derived macrophages: an opportunity for an in vitro drug screening assay, In Vitro Models 1 (2022) 365–383, https://doi.org/10.1007/s44164-022-00035-8.
[50] D. Paolino, A. Vero, D. Cosco, T.M.G. Pecora, S. Cianciolo, M. Fresta, R. Pignatello, Improvement of oral bioavailability of curcumin upon microencapsulation with methacrylic copolymers, Front. Pharmacol. 7-2016 (2016), https://doi.org/10.3389/fphar.2016.00485.
[51] Y. Ferrara, D. Latino, A. Costagliola di Polidoro, A. Oliver, A. Sarnella, M.G. Caprio, L. Cerchia, M. Ruvo, A. Sandomenico, A. Zannetti, A novel therapeutic approach targeting PD-L1 in HNSCC and bone marrow-derived mesenchymal stem cells hampers pro-metastatic features in vitro: perspectives for blocking tumor-stroma communication and signaling, Cell Commun. Signal 23 (2025) 74, https://doi.org/10.1186/s12964-025-02073-7.
[52] S. Scicchitano, A. Gagliardi, N. Ambrosio, E. Vecchio, C. Garofalo, A.M. Battaglia, F.S. Costanzo, M.C. Faniello, D. Cosco, Exploring the effects of paclitaxel-loaded zein nanoparticles on human ovarian carcinoma cells, Sci. Rep. 15 (2025) 10553, https://doi.org/10.1038/s41598-025-90840-4.
[53] A.A.M. Kämpfer, P. Urbán, S. Gioria, N. Kanase, V. Stone, A. Kinsner-Ovaskainen, Development of an in vitro co-culture model to mimic the human intestine in healthy and diseased state, Toxicol. in Vitro 45 (2017) 31–43, https://doi.org/10.1016/j.tiv.2017.08.011.
[54] B. Park, G. Han, D.Y. Jin, K.C. Gil, D. Shin, J. Lee, J.Y. Park, H. Jang, D. Park, S. Lee, K. Kim, Y. Yang, Y. Kim, J.S. Kim, S.H. Kim, M.K. Shim, Mucoadhesive mesalamine prodrug nanoassemblies to target intestinal macrophages for the treatment of inflammatory bowel disease, ACS Nano 18 (2024) 16297–16311, https://doi.org/10.1021/acsnano.4c05544.
[55] C. D'Alterio, A. Zannetti, A.M. Trotta, C. Ieranò, M. Napolitano, G. Rea, A. Greco, P. Maiolino, S. Albanese, G. Scognamiglio, New CXCR4 antagonist peptide R (pep R) improves standard therapy in colorectal cancer, Cancers (Basel) 12 (2020) 1952, https://doi.org/10.3390/cancers12071952.
[56] A. Simões, M. Miranda, C. Cardoso, F. Veiga, C. Vitorino, Rheology by design: a regulatory tutorial for analytical method validation, Pharmaceutics 12 (2020) 820, https://doi.org/10.3390/pharmaceutics12090820.
[57] M. Pourbakhsh, M. Jabraili, M. Akbari, M. Jaymand, R. Jahanban Esfahlan, Poloxamer-based drug delivery systems: frontiers for treatment of solid tumors, Mater. Today Bio 32 (2025) 101727, https://doi.org/10.1016/j.mtbio.2025.101727.
[58] A. Aprodu, J. Mantaj, B. Raimi-Abraham, D. Vllasaliu, Evaluation of a methylcellulose and hyaluronic acid hydrogel as a vehicle for rectal delivery of biologics, Pharmaceutics 11 (2019), https://doi.org/10.3390/pharmaceutics11030127.
[59] E.J. Ricci, M.V.L. Bentley, M. Farah, R.E.S. Bretas, J.M. Marchetti, Rheological characterization of Poloxamer 407 lidocaine hydrochloride gels, Eur. J. Pharm. Sci. 17 (2002) 161–167, https://doi.org/10.1016/S0928-0987(02)00166-5.
[60] G. Stojkov, Z. Niyazov, F. Picchioni, R.K. Bose, Relationship between structure and rheology of hydrogels for various applications, Gels 7 (2021), https://doi.org/10.3390/gels7040255.
[61] G.G. Pereira, F.A. Dimer, S.S. Guterres, C.P. Kechinski, J.E. Granada, N.S. M. Cardozo, Formulation and characterization of poloxamer 407®: thermoreversible gel containing polymeric microparticles and hyaluronic acid, Quim Nova 36 (2013) 1121–1125, https://doi.org/10.1590/S0100-40422013000800008.
[62] A. Saleem, F. ud Din, Z. Ali, F. Zahid, A.H. Alamri, A.A. Lahiq, T. Alqahtani, H. M. Alharbi, Development and evaluation of regorafenib loaded liquid suppository for rectal delivery: in vitro, in vivo analyses, J. Drug Deliv. Sci. Technol. 91 (2024) 105239, https://doi.org/10.1016/j.jddst.2023.105239.
[63] I.S. Bayer, Recent advances in mucoadhesive interface materials, mucoadhesion characterization, and technologies, Adv. Mater. Interfaces 9 (2022) 2200211, https://doi.org/10.1002/admi.202200211.
[64] S. Voci, A. Gagliardi, E. Giuliano, M.C. Salvatici, A. Procopio, D. Cosco, In vitro mucoadhesive features of gliadin nanoparticles containing thiamine hydrochloride, Pharmaceutics 16 (2024), https://doi.org/10.3390/pharmaceutics16101296.
[65] L. Garcia-del Rio, P. Diaz-Rodriguez, M. Landin, New tools to design smart thermosensitive hydrogels for protein rectal delivery in IBD, Mater. Sci. Eng. C 106 (2020) 110252, https://doi.org/10.1016/j.msec.2019.110252.
[66] M.A. Akl, H.R. Ismael, F.I. Abd Allah, A.A. Kassem, A.M. Samy, Tolmetin sodium-loaded thermosensitive mucoadhesive liquid suppositories for rectal delivery; strategy to overcome oral delivery drawbacks, Drug Dev. Ind. Pharm. 45 (2019) 252–264, https://doi.org/10.1080/03639045.2018.1534858.
[67] N.S. Barakat, In vitro and in vivo characteristics of a thermogelling rectal delivery system of etodolac, AAPS PharmSciTech 10 (2009) 724–731, https://doi.org/10.1208/s12249-009-9261-y.
[68] Z. Guo, Y. Bai, Z. Zhang, H. Mei, J. Li, Y. Pu, N. Zhao, W. Gao, F. Wu, B. He, Thermosensitive polymer hydrogel as a physical shield on colonic mucosa for colitis treatment, J. Mater. Chem. B 9 (2021) 3874–3884, https://doi.org/10.1039/D1TB00499A.
[69] S. Van Hemelryck, J. Dewulf, H. Niekus, M. van Heerden, B. Ingelse, R. Holm, E. Mannaert, P. Langguth, In vitro evaluation of poloxamer in situ forming gels for bedaquiline fumarate salt and pharmacokinetics following intramuscular injection in rats, Int. J. Pharm.: X 1 (2019) 100016, https://doi.org/10.1016/j.ijpx.2019.100016.

[70] C.Y. Gong, S. Shi, X.Y. Peng, B. Kan, L. Yang, M.J. Huang, F. Luo, X. Zhao, Y. Q. Wei, Z.Y. Qian, Biodegradable thermosensitive injectable PEG-PCL-PEG hydrogel for bFGF antigen delivery to improve humoral immunity, Growth Factors 27 (2009) 377–383, https://doi.org/10.3109/08977190903159938.
[71] Q.J. Wu, X.C. Zhu, X. Xiao, P. Wang, D.K. Xiong, C.Y. Gong, Y.S. Wang, L. Yang, Y. Q. Wei, A novel vaccine delivery system: biodegradable nanoparticles in thermosensitive hydrogel, Growth Factors 29 (2011) 290–297, https://doi.org/10.3109/08977194.2011.624517.
[72] Y. Yuan, Y. Cui, L. Zhang, H. Zhu, Y.S. Guo, B. Zhong, X. Hu, L. Zhang, X. Wang, L. Chen, Thermosensitive and mucoadhesive in situ gel based on poloxamer as new carrier for rectal administration of nimesulide, Int. J. Pharm. 430 (2012) 114–119, https://doi.org/10.1016/j.ijpharm.2012.03.054.
[73] E. Giuliano, E. Longo, A. Gagliardi, M.C. Salvatici, V. Gaetano, D. Cosco, Stable liposome–hydrogel composites as multistage drug delivery systems, J. Drug Deliv. Sci. Technol. 115 (2026) 107845, https://doi.org/10.1016/j.jddst.2025.107845.
[74] M. Zeeshan, H. Ali, S. Khan, S.A. Khan, B. Weigmann, Advances in orally-delivered pH-sensitive nanocarrier systems; an optimistic approach for the treatment of inflammatory bowel disease, Int. J. Pharm. 558 (2019) 201–214, https://doi.org/10.1016/j.ijpharm.2018.12.074.
[75] H.G. Choi, M.-K. Lee, M.H. Kim, C.-K. Kim, Effect of additives on the physicochemical properties of liquid suppository bases, Int. J. Pharm. 190 (1999) 13–19, https://doi.org/10.1016/S0378-5173(99)00225-2.
[76] H.G. Choi, J.H. Jung, J.M. Ryu, S.J. Yoon, Y.K. Oh, C.K. Kim, Development of in situ-gelling and mucoadhesive acetaminophen liquid suppository, Int. J. Pharm. 165 (1998) 33–44, https://doi.org/10.1016/S0378-5173(97)00386-4.
[77] S.A. Bernal-Chávez, S. Alcalá-Alcalá, D. Cerecedo, A. Ganem-Rondero, Platelet lysate-loaded PLGA nanoparticles in a thermo-responsive hydrogel intended for the treatment of wounds, Eur. J. Pharm. Sci. 146 (2020) 105231, https://doi.org/10.1016/j.ejps.2020.105231.
[78] A. El-Kamel, M. El-Khatib, Thermally reversible in situ gelling carbamazepine liquid suppository, Drug Deliv. 13 (2006) 143–148, https://doi.org/10.1080/10717540500316003.
[79] F. Al-Joufi, M. Elmowafy, N.K. Alruwaili, K.S. Alharbi, K. Shalaby, S.D. Alsharari, H.M. Ali, Mucoadhesive in situ rectal gel loaded with rifampicin: strategy to improve bioavailability and alleviate liver toxicity, Pharmaceutics 13 (2021), https://doi.org/10.3390/pharmaceutics13030336.
[80] H.G. Choi, Y.K. Oh, C.K. Kim, In situ gelling and mucoadhesive liquid suppository containing acetaminophen: enhanced bioavailability, Int. J. Pharm. 165 (1998) 23–32, https://doi.org/10.1016/S0378-5173(97)00385-2.
[81] M.M. Alam, F. Tasneem, A.K.L. Kabir, A.S.S. Rouf, Study of drug-drug and drug-food interactions of mesalazine through FTIR and DSC, Dhaka Univ, J. Pharm. Sci. 18 (2019) 257–269, https://doi.org/10.3329/dujps.v18i2.44466.
[82] I.B.C. Lima, L.C.G.A.I. Moreno, A.V. Peres, A.C.G. Santana, A. Carvalho, M. H. Chaves, L. Lima, R.W. Sousa, D. Dittz, H.M.L. Rolim, Nanoparticles obtained from zein for encapsulation of mesalazine, Pharmaceutics 14 (2022) 2830, https://doi.org/10.3390/pharmaceutics14122830.
[83] J.G. Pontes-Neto, T.R.F. Silva, F.O.S. Ribeiro, D.A. Silva, M.F.R. Soares, J.L. Soares-Sobrinho, Reconstitution as an alternative method for 5-aminosalicylic acid intercalation in layered double hydroxide for drug delivery, J. Therm. Anal. Calorim. 147 (2022) 3141–3149, https://doi.org/10.1007/s10973-021-10684-8.
[84] E.P. Raj, S. Anjali, P. Rajesh, S. Dash, Enhancing solubilization of Nebivolol hydrochloride through tuning pluronic F-127 with ionic surfactants: an experimental and theoretical investigation, J. Mol. Liq. (2024) 124343, https://doi.org/10.1016/j.molliq.2024.124343.
[85] M. Beiranvand, A review of the biological and pharmacological activities of mesalazine or 5-aminosalicylic acid (5-ASA): an anti-ulcer and anti-oxidant drug, Inflammopharmacology 29 (2021) 1279–1290, https://doi.org/10.1007/s10787-021-00856-1.
[86] M.H. Macedo, M. Dias Neto, L. Pastrana, C. Gonçalves, M. Xavier, Recent advances in cell-based in vitro models to recreate human intestinal inflammation, Adv. Sci. 10 (2023) 2301391, https://doi.org/10.1002/advs.202301391.
[87] Intestinal stem cells (ISCs): ISCs-derived organoids for disease modeling and therapy, Eur. Cell. Mater. 50 (2025) 84–86, https://doi.org/10.22203/eCM.v050a05.
[88] P. Xue, L. Wang, J. Xu, J. Liu, X. Pan, Y. Zhao, H. Xu, Temperature-sensitive hydrogel for rectal perfusion improved the therapeutic effect of Kangfuxin liquid on DSS-induced ulcerative colitis mice: the inflammation alleviation and the colonic mucosal barriers repair, Int. J. Pharm. 589 (2020) 119846, https://doi.org/10.1016/j.ijpharm.2020.119846.
[89] V. Kant, A. Gopal, D. Kumar, A. Gopalkrishnan, N.N. Pathak, N.P. Kurade, S. K. Tandan, D. Kumar, Topical pluronic F-127 gel application enhances cutaneous wound healing in rats, Acta Histochem. 116 (2014) 5–13, https://doi.org/10.1016/j.acthis.2013.04.010.
[90] M. Le Fur, I.Y. Zhou, O. Catalano, P. Caravan, Toward molecular imaging of intestinal pathology, Inflamm. Bowel Dis. 26 (2020) 1470–1484, https://doi.org/10.1093/ibd/izaa213.
[91] B. Chassaing, J.D. Aitken, M. Malleshappa, M. Vijay-Kumar, Dextran sulfate sodium (DSS)-induced colitis in mice, Curr. Protoc. Immunol. 104 (2014) 15.25.1–15.25.14, https://doi.org/10.1002/0471142735.im1525s104.
[92] C.F. Krieglstein, W.H. Cerwinka, F.S. Laroux, M.B. Grisham, G. Schürmann, M. Brüwer, D.N. Granger, Role of appendix and spleen in experimental colitis, J. Surg. Res. 101 (2001) 166–175, https://doi.org/10.1006/jsre.2001.6223.
[93] Y.J. Park, C.S. Yong, H.M. Kim, J.D. Rhee, Y.K. Oh, C.K. Kim, H.-G. Choi, Effect of sodium chloride on the release, absorption and safety of diclofenac sodium delivered by poloxamer gel, Int. J. Pharm. 263 (2003) 105–111, https://doi.org/10.1016/S0378-5173(03)00362-4.
[94] J.M. Ryu, S.-J. Chung, M.-H. Lee, C.K. Kim, Chang-Koo Shim, Increased bioavailability of propranolol in rats by retaining thermally gelling liquid suppositories in the rectum, J. Control. Release 59 (1999) 163–172, https://doi.org/10.1016/S0168-3659(98)00189-8.
[95] L. Zhao, F. Wang, Z. Cai, Q. Zhou, B. Chen, C. Zhang, H. Liu, L. Hong, T. Zhang, J. Zhong, W. Cui, Z. Wang, Improving drug utilization platform with injectable mucoadhesive hydrogel for treating ulcerative colitis, Chem. Eng. J. 424 (2021) 130464, https://doi.org/10.1016/j.cej.2021.130464.
[96] J. Sun, P. Xue, J. Liu, L. Huang, G. Lin, K. Ran, J. Yang, C. Lu, Y.-Z. Zhao, H.-L. Xu, Self-cross-linked hydrogel of cysteamine-grafted γ-polyglutamic acid stabilized tripeptide KPV for alleviating TNBS-induced ulcerative colitis in rats, ACS Biomater Sci. Eng. 7 (2021) 4859–4869, https://doi.org/10.1021/acsbiomaterials.1c00792.
[97] E. Guler, F.K.M. Abobakr, M.S. Bostan, M.S. Eroglu, M.E. Cam, Evaluation of the mesalazine-loaded nanoparticles-embedded BSA hydrogels for the ulcerative colitis treatment, 2024, https://doi.org/10.25135/acg.oc.171.2405.3240.
[98] S.N. Kuo, P.X. Wu, S.L. Huang, Y.C. Hsu, J.H. Huang, Thermo-responsive methylcellulose/hyaluronic acid–mesalamine hydrogel in targeted drug delivery for ulcerative colitis, RSC Adv. 15 (2025) 14126–14135, https://doi.org/10.1039/D5RA00216H.